JAK tyrosine kinases promote hierarchical activation of Rho and Rap modules of integrin activation

Alessio Montresor,[1,2] Matteo Bolomini-Vittori,[1] Lara Toffali,[1] Barbara Rossi,[1] Gabriela Constantin,[1] and Carlo Laudanna[1,2]

[1]Department of Pathology and Diagnostics, Division of General Pathology, School of Medicine, and [2]The Center for Biomedical Computing, University of Verona, Verona 37134, Italy

Lymphocyte recruitment is regulated by signaling modules based on the activity of Rho and Rap small guanosine triphosphatases that control integrin activation by chemokines. We show that Janus kinase (JAK) protein tyrosine kinases control chemokine-induced LFA-1– and VLA-4–mediated adhesion as well as human T lymphocyte homing to secondary lymphoid organs. JAK2 and JAK3 isoforms, but not JAK1, mediate CXCL12-induced LFA-1 triggering to a high affinity state. Signal transduction analysis showed that chemokine-induced activation of the Rho module of LFA-1 affinity triggering is dependent on JAK activity, with VAV1 mediating Rho activation by JAKs in a $G\alpha_i$-independent manner. Furthermore, activation of Rap1A by chemokines is also dependent on JAK2 and JAK3 activity. Importantly, activation of Rap1A by JAKs is mediated by RhoA and PLD1, thus establishing Rap1A as a downstream effector of the Rho module. Thus, JAK tyrosine kinases control integrin activation and dependent lymphocyte trafficking by bridging chemokine receptors to the concurrent and hierarchical activation of the Rho and Rap modules of integrin activation.

Introduction

Leukocyte recruitment is a concurrent ensemble of leukocyte behaviors, including tethering, rolling, firm adhesion, crawling, and transmigration (Ley et al., 2007). A central step is the integrin-mediated arrest, comprising a series of adhesive events, including increase of integrin affinity, valency, and binding stabilization altogether controlling cell avidity. In this context, modulation of LFA-1 (lymphocyte function-associated antigen 1) affinity is widely recognized as the prominent event in rapid leukocyte arrest induced by chemokines (Constantin et al., 2000; Giagulli et al., 2004; Kim et al., 2004; Bolomini-Vittori et al., 2009). Structural data predict that LFA-1 exists in at least three conformational states, differing both in their complete extension over the plasma membrane as well as in the arrangement of their headpiece corresponding to increased binding affinity for the ligands (Luo et al., 2007).

Regulation of integrin activation depends of a plethora of signaling proteins (Montresor et al., 2012). To date, signaling by Rho and Rap small GTPases is the best-studied mechanism of integrin activation by chemokines. In this context, we have recently proposed four criteria of experimental validation that should be systematically fulfilled to correlate signaling events to the modulation of integrin affinity under physiological conditions (Montresor et al., 2012). The criteria include (1) evaluation of signaling events in primary leukocytes, (2) evaluation of adhesion underflow conditions, (3) measurement of rapid kinetics of adhesion triggering (seconds or less), and (4) direct detection of heterodimer conformational changes. Accordingly, only a subset of signaling proteins involved in adhesion regulation was clearly demonstrated capable of regulating integrin affinity triggering by chemokines under physiological conditions (Montresor et al., 2012). Recently, we demonstrated that, in human primary T lymphocytes, chemokines control conformer-selective LFA-1 affinity triggering and in vivo homing by means of a signaling module based on the concurrent activity of RhoA, Rac1, and CDC42 small GTPases in turn controlling the function of PLD1 and PIP5K1C (phosphatidylinositol-4-phosphate 5-kinase, type I, γ; Bolomini-Vittori et al., 2009). At present,

A. Montresor, M. Bolomini-Vittori, and L. Toffali contributed equally to this paper.

Correspondence to Carlo Laudanna: carlo.laudanna@univr.it

Abbreviations used in this paper: HEV, high endothelial venule; GEF, guanine exchange factor; JAK, Janus kinase; NT, not treated; PtdIns(4,5)P_2, phosphatidylinositol 4,5-bisphosphate; PTK, protein tyrosine kinase; PTx, Pertussis toxin; TKIP, tyrosine kinase inhibitor peptide.

The Rockefeller University Press $30.00
J. Cell Biol. Vol. 203 No. 6 1003–1019
www.jcb.org/cgi/doi/10.1083/jcb.201303067

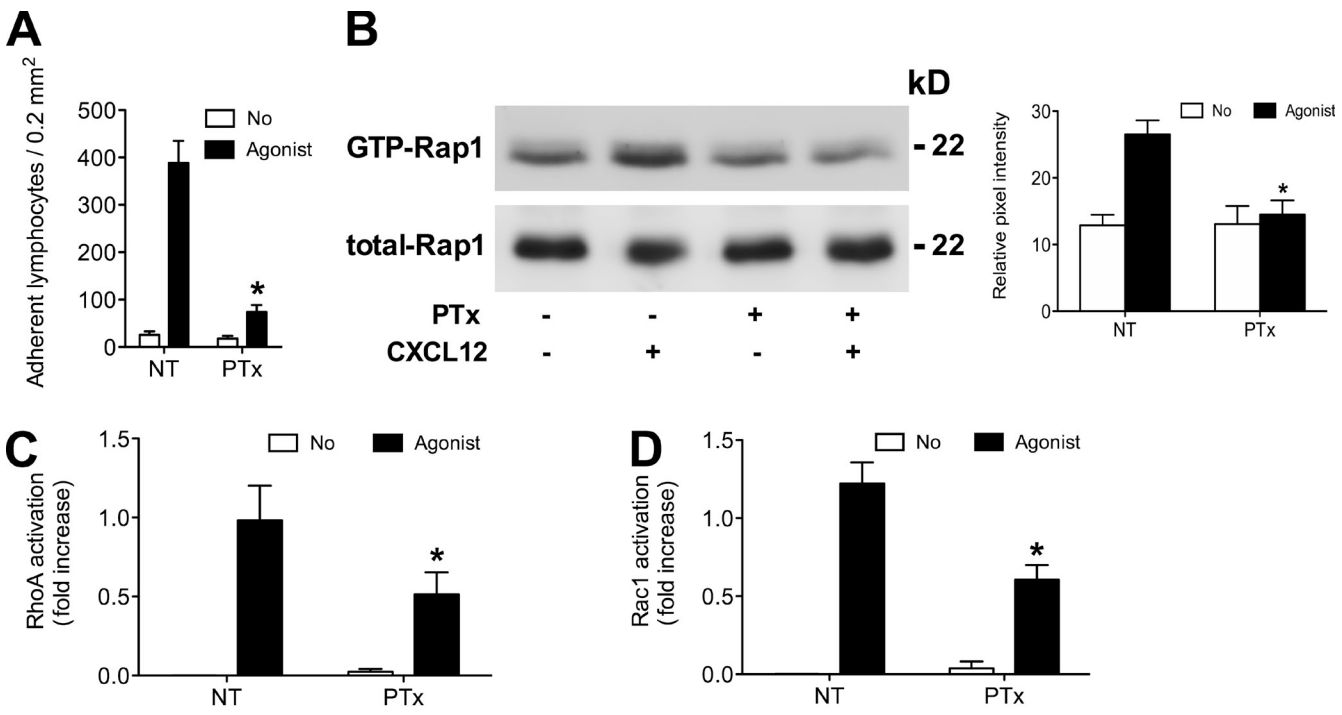

Figure 1. **Heterotrimeric Gα_i protein signaling is differently involved in Rap1A, RhoA, and Rac1 activation by CXCL12.** (A) Static adhesion assay to ICAM-1. Lymphocytes were treated with buffer (not treated [NT]) or 2 µg/ml pertussis toxin (PTx) for 2 h and stimulated with 0.2 µM CXCL12 (agonist); four experiments in triplicate. (B, left) Rap1A activation was measured by pull-down assay. Lymphocytes were treated as in A and stimulated with 0.2 µM CXCL12; representative experiment of three. (right) The relative ratio of the band intensity of GTP-Rap1A was normalized to the level of total Rap1A intensity. (C and D) G-LISA assay detecting RhoA (C) and Rac1 (D) activation. Lymphocytes were treated as in A and stimulated with 0.2 µM CXCL12 (agonist). The percentage of fold increase of the RhoA and Rac1 activation was normalized to the level of NT intensity; mean of three experiments. Error bars show SDs. *, $P < 0.01$, versus NT.

however, the upstream signaling mechanisms linking chemokine receptors to Rho module activation in the context of LFA-1 affinity triggering by arrest chemokines are unknown.

Chemokines control a range of cellular phenomena by means of signaling events classically related to heterotrimeric Gα_i protein transducing activity. Past data show that also members of the Janus kinase (JAK) family of protein tyrosine kinases (PTKs) are transducers of chemokine receptor signaling (Vila-Coro et al., 1999; Soriano et al., 2003; Soldevila et al., 2004; García-Zepeda et al., 2007). Indeed, although JAKs have been generally associated to cytokine signaling, mainly controlling the STAT pathway, evidence suggests that chemokine receptors interact with and activate JAKs (Soriano et al., 2003; Stein et al., 2003). JAK is a family of cytosolic tyrosine kinases including four members: JAK1, JAK2, JAK3, and TYK2 (tyrosine kinase 2). Each isoform contains a conserved kinase domain and a related, but catalytically inactivate, pseudokinase domain at the carboxyl terminus regulating the kinase activity. In spite of this knowledge, little is known about the role of JAKs in regulating signaling events leading to rapid integrin affinity triggering and dependent lymphocyte adhesion induced by arrest chemokines under physiological conditions.

In this study, we investigated the role of JAKs as chemokine receptor upstream transducers controlling integrin activation in human primary T lymphocytes. We show that JAK2 and JAK3 are activated by the CXCR4 ligand CXCL12 and control LFA-1 affinity maturation in human primary T lymphocytes. JAKs also mediate VLA-4 activation. Accordingly, JAK2 and JAK3 are pivotal to T lymphocyte homing to secondary lymphoid organs. Importantly, we show that JAK2 and JAK3 mediate CXCL12-induced activation of the four proadhesive components of the Rho module of LFA-1 affinity triggering, namely RhoA, Rac1, PLD1, and PIP5K1C. We also show that the Rho guanine exchange factor (GEF) VAV1 is tyrosine phosphorylated by JAKs, mediates RhoA and Rac1 activation by CXCL12, and is involved in LFA-1 affinity triggering. Surprisingly, we found that JAK2 and JAK3 also mediate Rap1A (Ras-related protein 1A) activation by CXCL12. We provide evidence showing that JAK-mediated activation of Rap1A is dependent on RhoA and PLD1, thus establishing Rap1A as a novel downstream effector of Rho to integrin activation. Our results characterize the very upstream mechanism of LFA-1 affinity triggering by chemokines and show that JAK tyrosine kinases along with Rho and Rap small GTPases generate an integrated, hierarchical signaling module globally controlling integrin activation and dependent lymphocyte trafficking.

Results

JAK2 and JAK3 are rapidly activated by CXCL12 and control LFA-1–mediated adhesion of human primary T lymphocytes

Blockade of heterotrimeric Gα_i proteins by Pertussis toxin (PTx) was originally shown to prevent lymphocyte in vivo homing (Bargatze and Butcher, 1993). However, although we

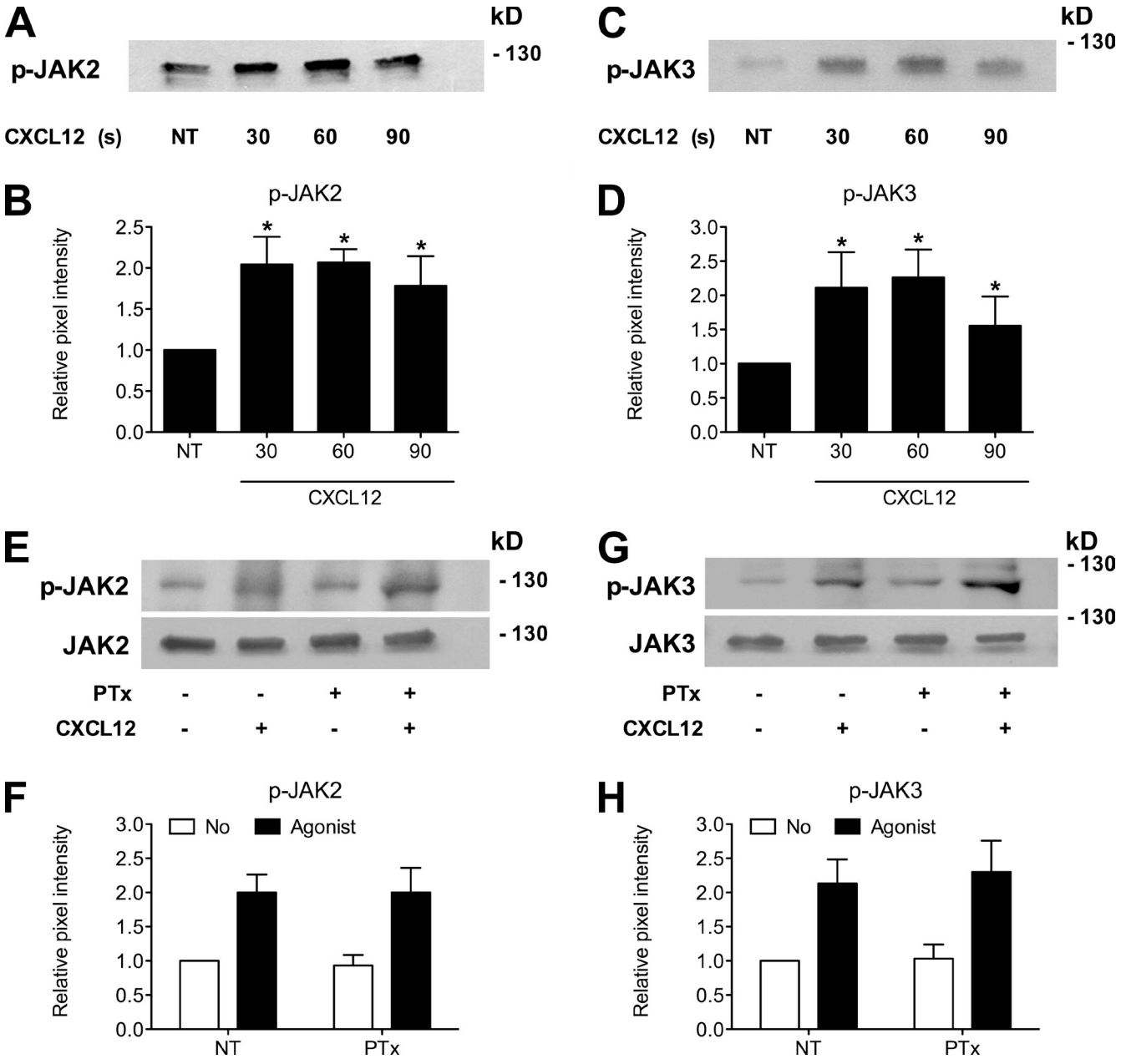

Figure 2. **CXCL12 rapidly triggers JAK2 and JAK3 activation independently of heterotrimeric $G\alpha_i$ protein signaling.** (A) Time course of JAK2 phosphorylation. Lymphocytes were treated with buffer (NT) or with 0.2 μM CXCL12 for the indicated times. Lysates were immunoprecipitated with antiphosphotyrosine antibody and probed with the anti-JAK2 or anti-JAK3 antibody (C); representative experiment of three. (B) Quantification of immunoreactive bands. The relative ratio of the band intensity of phospho-JAK2 was normalized to the level of NT. Mean values of three experiments. (C) Time course of JAK3 phosphorylation. Lymphocytes were treated as in A; representative experiment of six. (D) Quantification of immunoreactive bands. The relative ratio of the band intensity of phospho-JAK3 was normalized as in B. Mean values of three experiments. (E–H) JAK PTK activation is independent of heterotrimeric $G\alpha_i$ proteins. Lymphocytes were treated with buffer (NT) or 2 μg/ml pertussis toxin (PTx) for 2 h and stimulated with 0.2 μM CXCL12. Lysates were immunoprecipitated as in A. (E and G) Immunoblot of phospho-JAK2 (E) and phospho-JAK3 (G). (F and H) Representative experiment of three for each protein. Quantification of immunoreactive bands. The relative ratio of the band intensity of phospho-JAK2 (F) and phospho-JAK3 (H) was normalized to the level of NT intensity. Mean values of three experiments for each protein. Error bars show SDs. *, $P < 0.01$, versus NT.

verified that PTx completely inhibits human T lymphocyte in vitro adhesion by CXCL12 (Fig. 1 A), we surprisingly found that activation of Rap1A and Rho small GTPases by CXCL12 is differently affected by PTx, with Rap1A activation totally inhibited (Fig. 1 B), whereas RhoA and Rac1 activation only partially affected by PTx treatment (Fig. 1, C and D). This suggests that an interplay between different receptor transducers controls Rho and Rap signaling cascade triggering by chemokine receptors. We, thus, hypothesized that JAKs could be involved in signaling events leading to integrin triggering by chemokines. To evaluate whether JAKs are involved in LFA-1 activation by chemokines, we first verified JAK activation by CXCL12, detected as tyrosine autophosphorylation (Feng et al., 1997; Zhou et al., 1997). In human T lymphocytes, both JAK2 (Fig. 2, A and B) and JAK3 (Fig. 2, C and D) were rapidly phosphorylated upon CXCL12 stimulation, with kinetics consistent with rapid LFA-1

activation by chemokines. Interestingly, JAK1 was found not phosphorylated, suggesting an isoform-selective involvement of JAKs in CXCL12-triggered signaling (unpublished data). Notably, PTx treatment did not affect JAK2 and JAK3 phosphorylation triggered by CXCL12, thus suggesting a heterotrimeric $G\alpha_i$ protein–independent mechanism of JAK activation by chemokines (Fig. 2, E–H). We then evaluated whether JAK2 and JAK3 mediate LFA-1–dependent adhesion in human T lymphocytes. We first tested the capability of two inhibitors, AG490 (JAKs inhibitor) and WHI-P154, (JAK3-selective inhibitor), to block JAK activation. AG490 and WHI-P154 completely prevented CXCL12-triggered tyrosine autophosphorylation of both JAK2 and JAK3 (Fig. 3, A and B). As an additional approach, based on a different mechanism of inhibition, we designed a P1 (Penetratin-1)-coupled peptide, carrying the already described tyrosine kinase inhibitor peptide (TKIP) sequence (Flowers et al., 2004), blocking selectively JAK2 autophosphorylation and activation. The fusion P1-TKIP Trojan peptide consistently reduced CXCL12-triggered tyrosine phosphorylation of both JAK2 and JAK3 (Fig. 3, A and B). Notably, P1-TKIP strongly decreased both JAK2 and JAK3 phosphotyrosine levels (Fig. 3, A and B), even if it was designed from a JAK2-selective sequence. However, this is not completely unexpected because JAK2 and JAK3 may activate reciprocally by transphosphorylation (Vila-Coro et al., 1999; Matsuda et al., 2004). Importantly, pretreatment with the inhibitors did not alter the expression of CXCR4 (Fig. 3 C, left) nor of LFA-1 (Fig. 3 C, right) and did not affect cell viability (not depicted). Collectively, these data show that JAK2 and JAK3 are rapidly activated by CXCL12 and that AG490, WHI-P154, and P1-TKIP are suitable inhibitors to investigate the involvement of JAKs in chemokine proadhesive signaling.

We then investigated the involvement of JAKs in LFA-1–mediated static adhesion by chemokines. Pretreatment with AG490, WHI-P154, or with P1-TKIP inhibited, in a dose-dependent manner, CXCL12-triggered T lymphocyte adhesion to ICAM-1 (Fig. 3 D). The control P1 peptide was ineffective. To corroborate these results, we applied an siRNA-based approach. A pool of four different siRNAs specific for JAK2 or JAK3 was effective in reducing the expression level of each individual isoform (Fig. 4 A). Maximal efficacy of silencing was detected after 24 h from the nucleoporation, with a mean decrease of ~92 and 76% for JAK2 and JAK3, respectively (Fig. 4 B). Scrambled siRNAs were ineffective. Moreover, siRNA treatment did not affect the expression of CXCR4 nor of LFA-1 (Fig. 4 C). Importantly, lymphocytes showing low expression levels of JAK2 or JAK3 exhibited a consistently reduced CXCL12-triggered adhesion to ICAM-1, whereas cells treated with scrambled siRNAs adhered normally (Fig. 4 D).

We then tested in underflow conditions the involvement of JAKs in chemokine-triggered LFA-1–mediated lymphocyte arrest on ICAM-1. As shown in Fig. 5 (A–C), pretreatment with AG490, WHI-P154, or with P1-TKIP, but not with the P1 control peptide, prevented CXCL12-triggered rapid arrest, either quantified at 1 or 10 s of arrest time, thus possibly including events of adhesion stabilization. Inhibition of arrest was accompanied by a concomitant increase of rolling cells, as expected. Similar results were obtained in cells treated with JAK2- or JAK3-specific siRNAs. Lymphocytes showing down-regulated expression of JAK2 or JAK3 exhibited a highly defective arrest on ICAM-1, whereas scrambled siRNAs did not exert any effect (Fig. 5 D). Collectively, these in vitro findings demonstrate that JAK2 and JAK3 are rapidly activated by CXCL12 and are involved in CXCL12-triggered intracellular signaling leading to LFA-1–mediated arrest of human primary T lymphocytes.

JAK2 and JAK3 control lymphocyte in vivo homing to secondary lymphoid organs

We, then, analyzed the effect of blockade of JAK2 and JAK3 inhibition on human T lymphocyte arrest on high endothelial venules (HEVs) in exposed mouse Peyer's patches. We have previously reported that adoptively transferred human T cells efficiently roll and arrest in several mouse models of microcirculation (Battistini et al., 2003; Piccio et al., 2005; Bolomini-Vittori et al., 2009). Moreover, we verified that mouse CCL21 does trigger LFA-1 affinity and mediated adhesion in human primary lymphocytes (Fig. S1, A–C). Pretreatment with AG490, WHI-P154, or P1-TKIP did not affect T lymphocyte tethering or rolling. However, all three inhibitors consistently blocked rapid arrest of T lymphocytes on HEVs (Fig. 5, E–G). These data definitively confirm the previous in vitro findings and fully support the physiological regulatory relevance of JAK2 and JAK3 in lymphocyte trafficking.

Chemokine-triggered LFA-1 affinity modulation is controlled by JAK2 and JAK3

To further define the regulatory role of JAK2 and JAK3 in LFA-1 activation, we assessed the effect of JAK2 and JAK3 blockade on CXCL12-induced LFA-1 conformational changes corresponding to increased affinity. JAK inhibition by AG490 (Fig. 6 A), by P1-TKIP peptide (Fig. 6 B) or by WHI-P154 (Fig. 6 C), almost completely prevented CXCL12-induced transition of LFA-1 to extended conformations recognized by the reporter monoclonal antibodies KIM127 (Fig. 6, A–C, left) and 327C (Fig. 6, A–C, right) corresponding to the low intermediate and high affinity states, respectively, supporting the crucial role of JAK2 and JAK3 in the CXCL12-triggered LFA-1 affinity modulation. Data obtained with chemical or peptide inhibitors were further confirmed in cells treated with JAK2- or JAK3-specific siRNAs. Lymphocytes showing down-regulated expression of JAK2 or JAK3 displayed defective triggering of LFA-1 to low intermediate (Fig. 6 D, left) and high affinity (Fig. 6 D, right) states induced by CXCL12, whereas the scrambled siRNAs had no effect. Altogether, these data establish, for the first time, JAK2 and JAK3 as critical signaling events mediating CXCL12-induced LFA-1 affinity activation.

Chemokine-triggered VLA-4–mediated adhesion is controlled by JAK2 and JAK3

To test whether the role of JAKs was integrin specific, we also evaluated the effect of JAK inhibition on VLA-4–mediated adhesion. As shown in Fig. S2 (A–D), in static adhesion assays on VCAM-1, JAK inhibition by inhibitors and by siRNA treatment consistently prevented rapid lymphocyte static adhesion

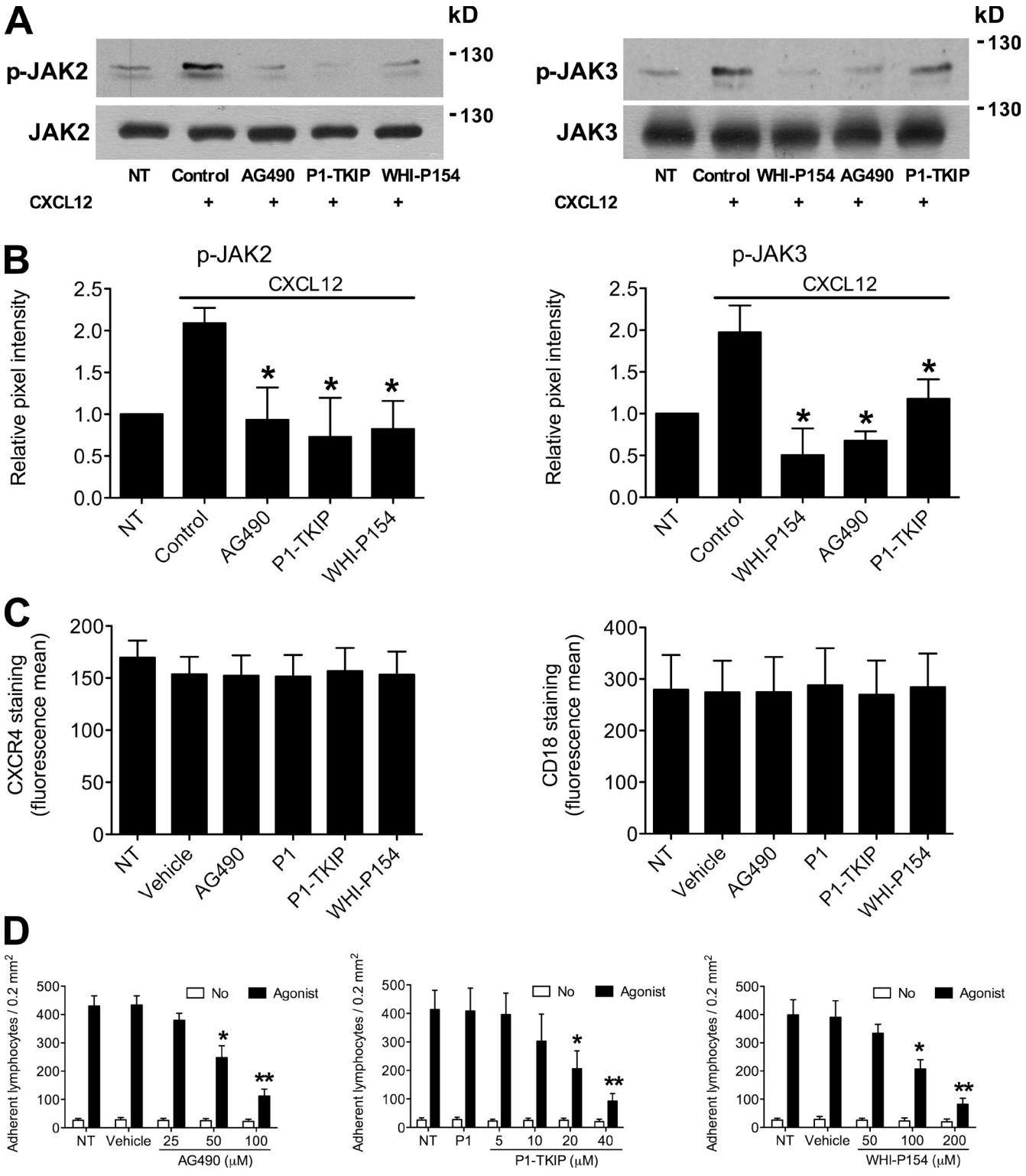

Figure 3. **JAK2 and JAK3 control CXCL12-triggered LFA-1–mediated static adhesion to ICAM-1 of human primary T lymphocytes.** (A) Effect of JAK inhibitors on JAK2 and JAK3 activation. Lymphocytes were treated with buffer (NT and control), 100 μM AG490, 40 μM P1-TKIP, or 200 μM WHI-P154 for 1 h and stimulated with 0.2 μM CXCL12 for 60 s. Lysates were immunoprecipitated with antiphosphotyrosine antibody and probed with anti-JAK2 (left) or anti-JAK3 antibody (right). The expression level of each protein was assessed in whole-cell lysates with anti-JAK2 or anti-JAK3 antibodies; representative experiment of three. (B) Quantification of immunoreactive bands. The relative ratio of the band intensity of phospho-JAK2 (left) and phospho-JAK3 (right) was normalized to the level of NT intensity. Mean values of three experiments for each protein. *, $P < 0.01$, versus control. (C) Flow cytometry measurement of CXCR4 (left) and CD18 (right) expression. Lymphocytes were treated as described in A; four experiments. (D) Dose–response effect of JAK inhibition in a static adhesion assay. Lymphocytes were treated with buffer (NT), DMSO (vehicle), AG490 (left), Penetratin-1 (P1) or P1-TKIP (middle), or WHI-P154 (right) at the indicated doses and stimulated with buffer (no) or 0.2 μM CXCL12 (agonist). Four experiments in triplicate. *, $P < 0.01$, versus vehicle or P1; **, $P < 0.001$, versus vehicle or P1. Error bars show SDs.

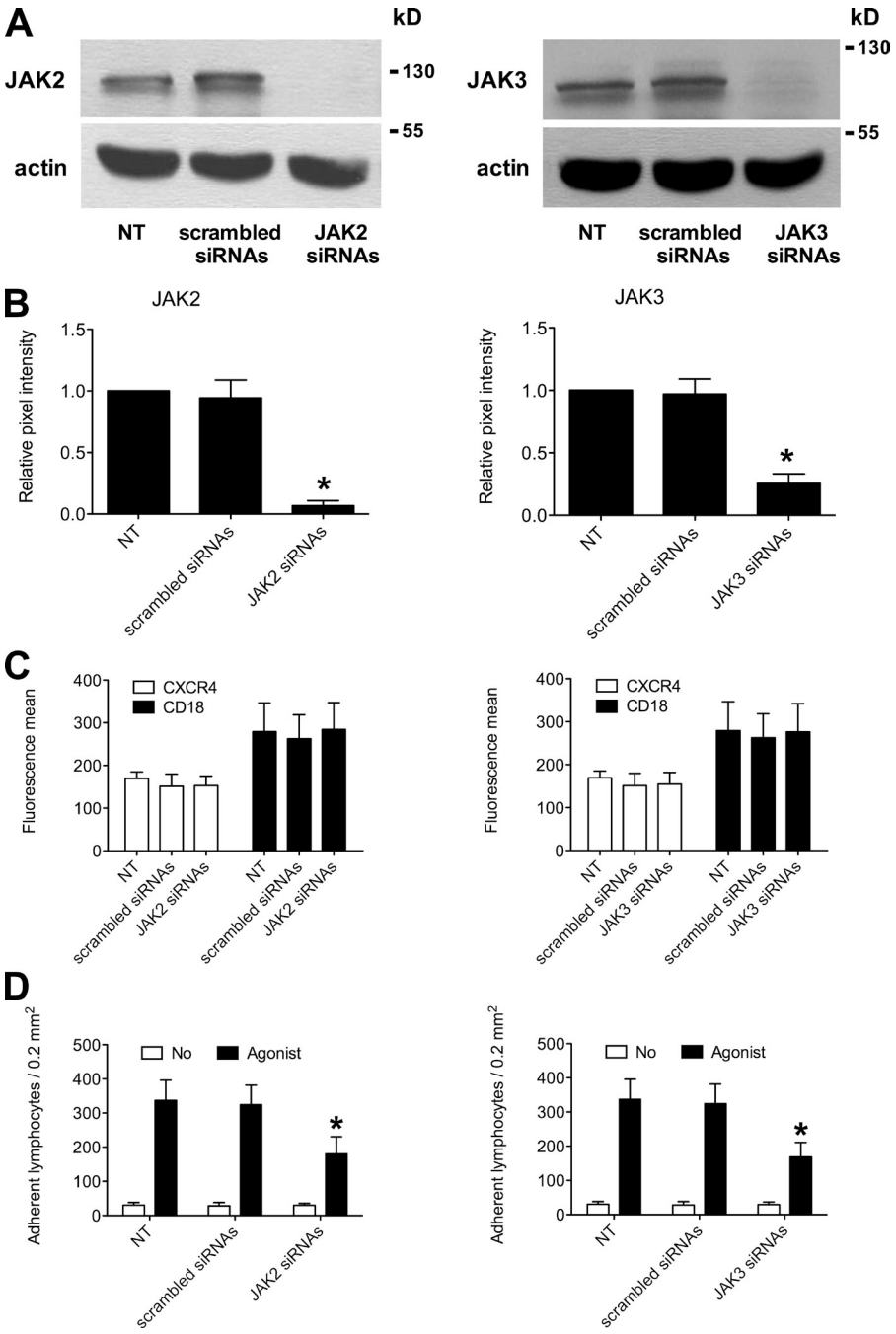

Figure 4. **Human primary T lymphocytes lacking of JAK2 or JAK3 display reduced CXCL12-triggered adhesion to ICAM-1.** (A) Immunoblot evaluation of JAK2 and JAK3 expression; lymphocytes were electroporated with a pool of four scrambled or JAK2 (left)- or JAK3 (right)-specific siRNAs and kept in culture for 24 h. Shown is the protein content compared with actin. The expression level of each protein was assessed in whole-cell lysates with anti-JAK2 or anti-JAK3 antibodies and then with an antiactin antibody for the loading control; representative experiment of five. (B) Quantification of immunoreactive bands. The relative ratio of the band intensity of total JAK2 (left) and JAK3 (right) was normalized to the level of NT intensity. Mean values of five experiments. (C) Flow cytometry measurement of CXCR4 (left) and CD18 (right) expression. Lymphocytes were treated as described in A; five experiments. (D) Static adhesion assay to ICAM-1. Lymphocytes were treated as in A and stimulated with buffer (no) or 0.2 µM CXCL12 (agonist); five experiments in triplicate. Error bars show SDs. *, $P < 0.01$, versus scrambled siRNAs.

on VCAM-1 by CXCL12. These data were also confirmed in underflow adhesion assays (Fig. S2, E–G). Notably, JAK inhibition did not alter VLA-4 expression (unpublished data). Overall, the data suggest that JAKs are general regulators of integrin activation by chemokines.

JAK2 and JAK3 mediate chemokine-induced activation of RhoA and Rac1 small GTPases

We have previously shown that, in human primary T lymphocytes, the small GTPases RhoA and Rac1 mediate LFA-1 affinity triggering by CXCL12 (Bolomini-Vittori et al., 2009). However, the possibility that JAKs may link chemokine receptors to Rho activation was never addressed. Inhibition of JAK2 and JAK3 by chemical inhibitors, P1-coupled blocking peptide, or by siRNAs consistently reduced activation of both RhoA and Rac1 triggered by CXCL12, as measured by pull-down assays (Fig. 7 A and Fig. S4, A and B). We also confirmed these results with a different approach, by taking advantage of two monoclonal antibodies that specifically recognize RhoA and Rac1 in a GTP-bound state coupled to single-cell image analysis. ImageStream analysis confirmed that JAK inhibition consistently prevents GDP–GTP exchange on RhoA and Rac1, reducing the percentage of cells containing activated RhoA and Rac1 (Fig. 7, B and C). Notably, simultaneous treatment with PTx and JAK inhibitors totally inhibited RhoA and

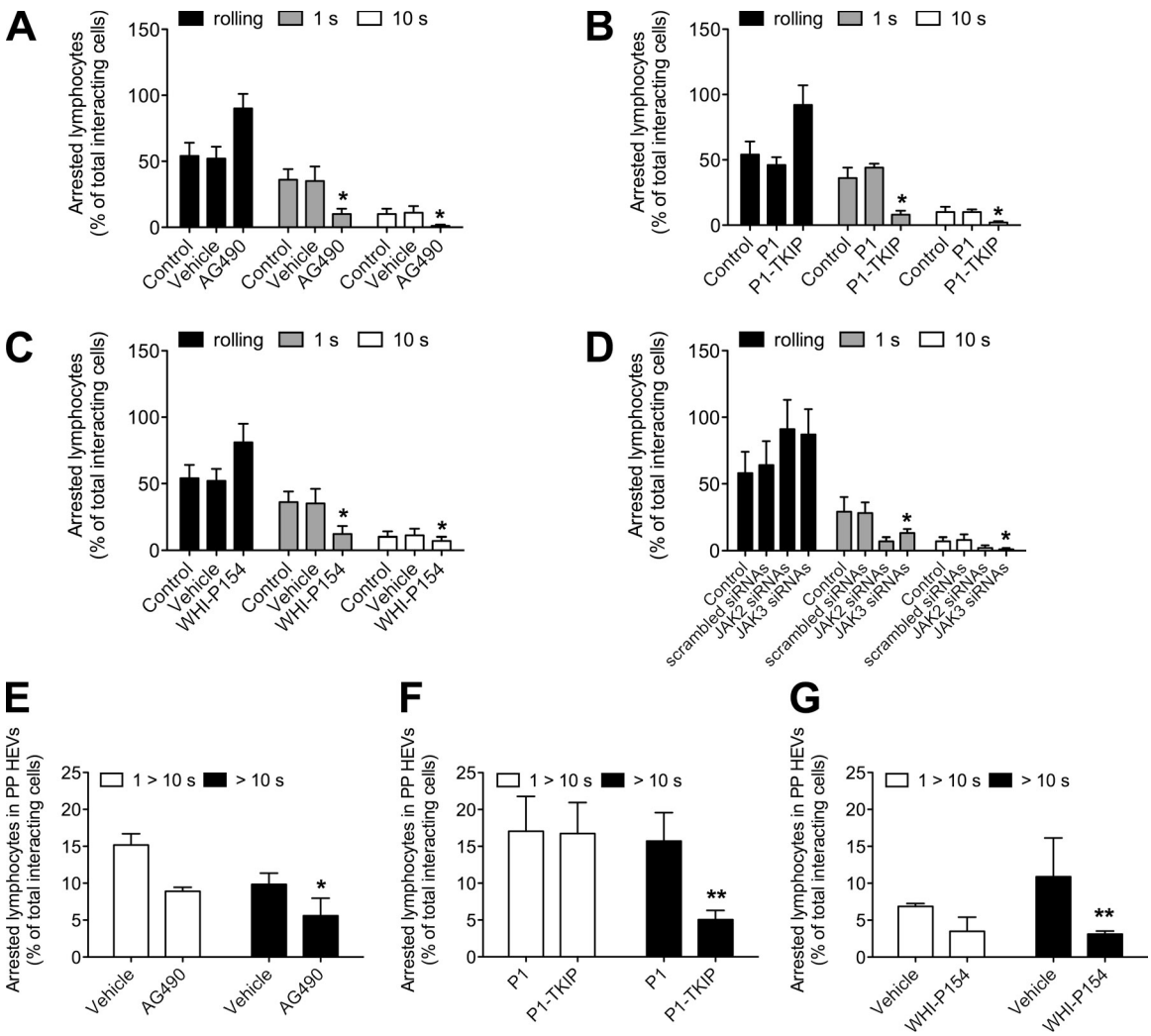

Figure 5. **JAK2 and JAK3 regulate CXCL12-triggered underflow arrest on ICAM-1 and homing to secondary lymphoid organs of human primary T lymphocytes.** Underflow adhesion assays. (A) Lymphocytes were treated with buffer (control), DMSO (vehicle), or 100 µM AG490 for 1 h; three experiments. Error bars show SDs. *, $P < 0.01$, versus vehicle. (B) Lymphocytes were treated with buffer (control), 40 µM Penetratin-1 (P1), or P1-TKIP for 1 h; three experiments. Error bars show SDs. *, $P < 0.01$, versus P1. (C) Lymphocytes were treated with buffer (control), DMSO (vehicle), or 200 µM WHI-P154 for 1 h; three experiments. Error bars show SDs. *, $P < 0.01$, versus vehicle. (D) Lymphocytes were electroporated with the pool of four scrambled or JAK2- or JAK3-specific siRNAs and kept in culture for 24 h; four experiments. Error bars show SDs. *, $P < 0.01$, versus scrambled siRNAs. In vivo homing to mouse Peyer's patches. Human primary T lymphocytes were injected in the mouse tail vein, and the cell behavior on HEVs was analyzed in exteriorized mouse Peyer's patches (PP). (E) Lymphocytes were treated as in A. (F) Lymphocytes were treated as in B. (G) Lymphocytes were as in C. Shown are percentages of arrested cells for the indicated times on total interacting cells. Values are means of four to five experiments. (E–G) Error bars show SEMs. *, $P < 0.05$; **, $P < 0.01$.

Rac1 activation by CXCL12, clearly suggesting concurrency between heterotrimeric $G\alpha_i$ proteins and JAK signaling events (Fig. 7 D). These data collectively demonstrate that JAK2 and JAK3 link CXCR4 to the activation of RhoA and Rac1 small GTPases, thus eliciting the signaling cascade controlling LFA-1 affinity modulation.

JAK2 and JAK3 mediate chemokine-induced activation of PLD1 and PIP5K1C

The RhoA and Rac1 downstream effectors PLD1 and PIP5K1C mediate CXCL12-triggered transition to LFA-1 high affinity state (Bolomini-Vittori et al., 2009). Notably, PLD1 and PIP5K1C can be also activated by alternative mechanisms (Cockcroft et al., 1994; Siddiqi et al., 2000; Krauss et al., 2003; Jarquin-Pardo et al., 2007; Oh et al., 2007; Sun et al., 2008), although a functional relationship between JAKs and PLD1 or PIP5K1C activation was never demonstrated. Thus, considering the role of JAKs in controlling RhoA and Rac1 activation, we tested whether JAKs could also control the activation of PLD1 and PIP5K1C. Pretreatment with AG490 or WHI-P154 strongly reduced PLD1 activity upon CXCL12 stimulation; similar results were also obtained with the P1-TKIP peptide, whereas the control P1 peptide did not exert any effect (Fig. 8 A). Moreover, inhibition of JAK2 or JAK3 effectively decreased phosphatidylinositol 4,5-bisphosphate ($PtdIns(4,5)P_2$), but not phosphatidylinositol and $PtdIns(4)P_2$, plasma membrane accumulation induced by CXCL12 (Fig. 8 B), indicating specific blockade of phosphatidylinositol 4-phosphate 5-kinase activity. Altogether, these data show that the entire signaling cascade comprising the Rho module of LFA-1 affinity triggering by

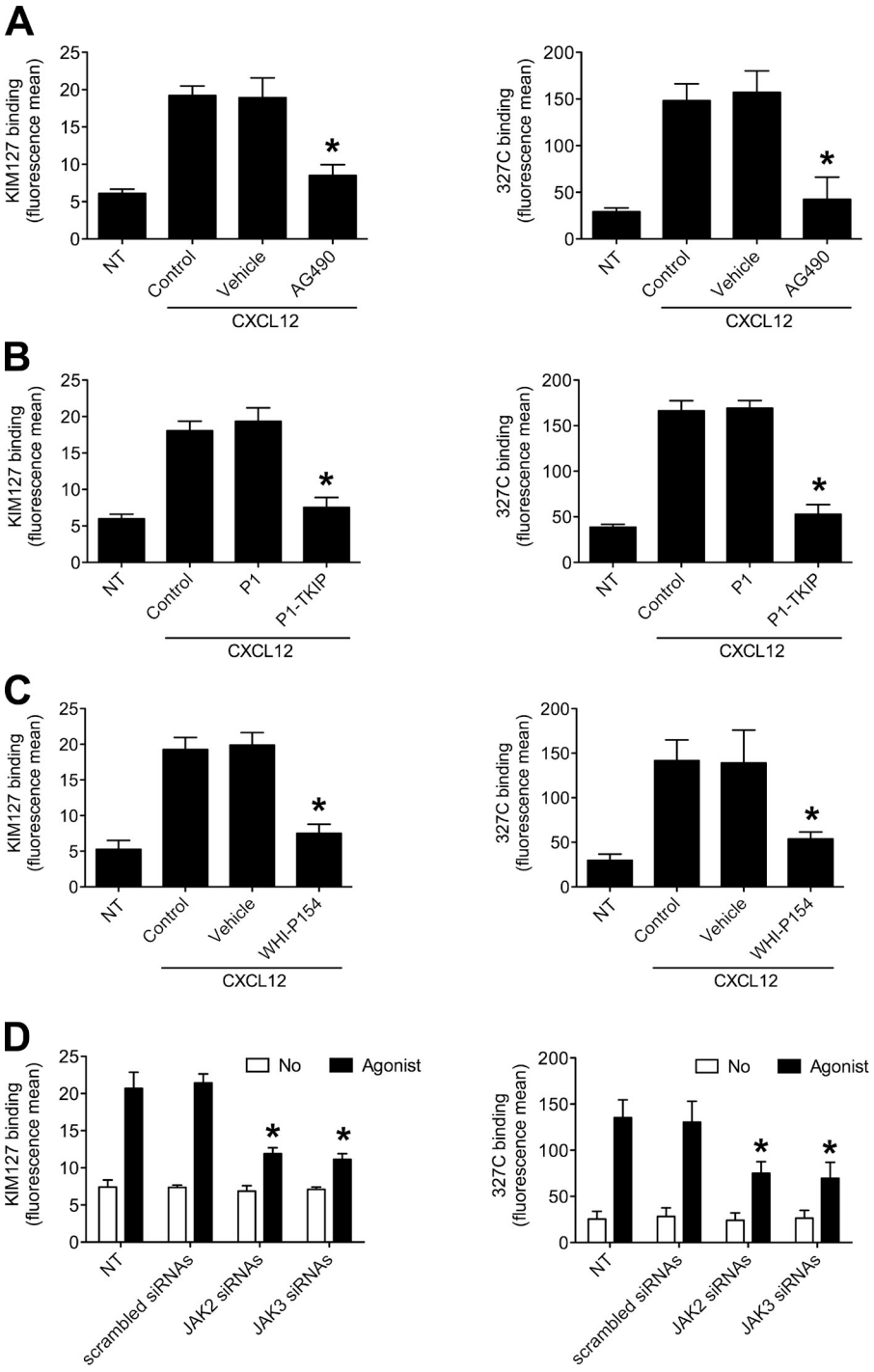

Figure 6. **JAK2 and JAK3 mediate LFA-1 affinity triggering by CXCL12.** (A) Lymphocytes were treated for 1 h with buffer (NT and control), DMSO (vehicle), or 100 µM AG490 and stimulated with 0.2 µM CXCL12. Different LFA-1 conformers were detected with the antibodies KIM127, detecting low-intermediate affinity state (left), or 327C, detecting high affinity state (right); five experiments in duplicate. *, $P < 0.01$, versus vehicle. (B) Lymphocytes were treated for 1 h with buffer (NT and control) or with 40 µM Penetratin-1 (P1) or P1-TKIP and stimulated with 0.2 µM CXCL12. Different LFA-1 conformers were detected as in A; five experiments in duplicate. *, $P < 0.01$, versus P1. (C) Lymphocytes were treated for 1 h with buffer (NT and control), DMSO (vehicle), or 200 µM WHI-P154 and stimulated with 0.2 µM CXCL12. Different LFA-1 conformers were detected as in A; four experiments in duplicate. *, $P < 0.01$, versus vehicle. (D) Lymphocytes were electroporated with the pool of four scrambled, JAK2- or JAK3-specific siRNAs, kept in culture for 24 h, and stimulated with buffer (no) or 0.2 µM CXCL12 (agonist). Different LFA-1 conformers were detected as in A; four experiments in duplicate. *, $P < 0.01$, versus scrambled siRNAs. Error bars show SDs.

chemokines is controlled by the upstream kinase activity of JAK2 and JAK3.

VAV1 mediates LFA-1 affinity triggering and Rho activation by JAK PTKs

The previous data imply that JAKs may activate one or more Rho GEFs involved in LFA-1 activation by chemokines. Rho GEFs critically involved in LFA-1 affinity triggering by chemokines are still unidentified. Because VAV1 was previously shown to be tyrosine phosphorylated by JAKs and involved in VLA-4–dependent adhesion (García-Bernal et al., 2005), we focused our attention on this Rho GEF. Lymphocytes nucleoporated with siRNA specific for VAV1 showed a consistent down modulated expression of VAV1 (Fig. 9, A and B). Importantly, lymphocytes displaying reduced VAV1 expression showed defective static as well as underflow adhesion on ICAM-1 (Fig. 9, C and D) along with defective LFA-1 affinity triggering (Fig. 9 E) and (Fig. 9 F) by CXCL12. Scrambled siRNA was ineffective. Moreover, we found that VAV1 was tyrosine phosphorylated by CXCL12 (Fig. 9, G and H) and that this phosphorylation was totally independent of $G\alpha_i$ signaling but almost completely dependent on JAK kinase activity (Fig. 9, I–L).

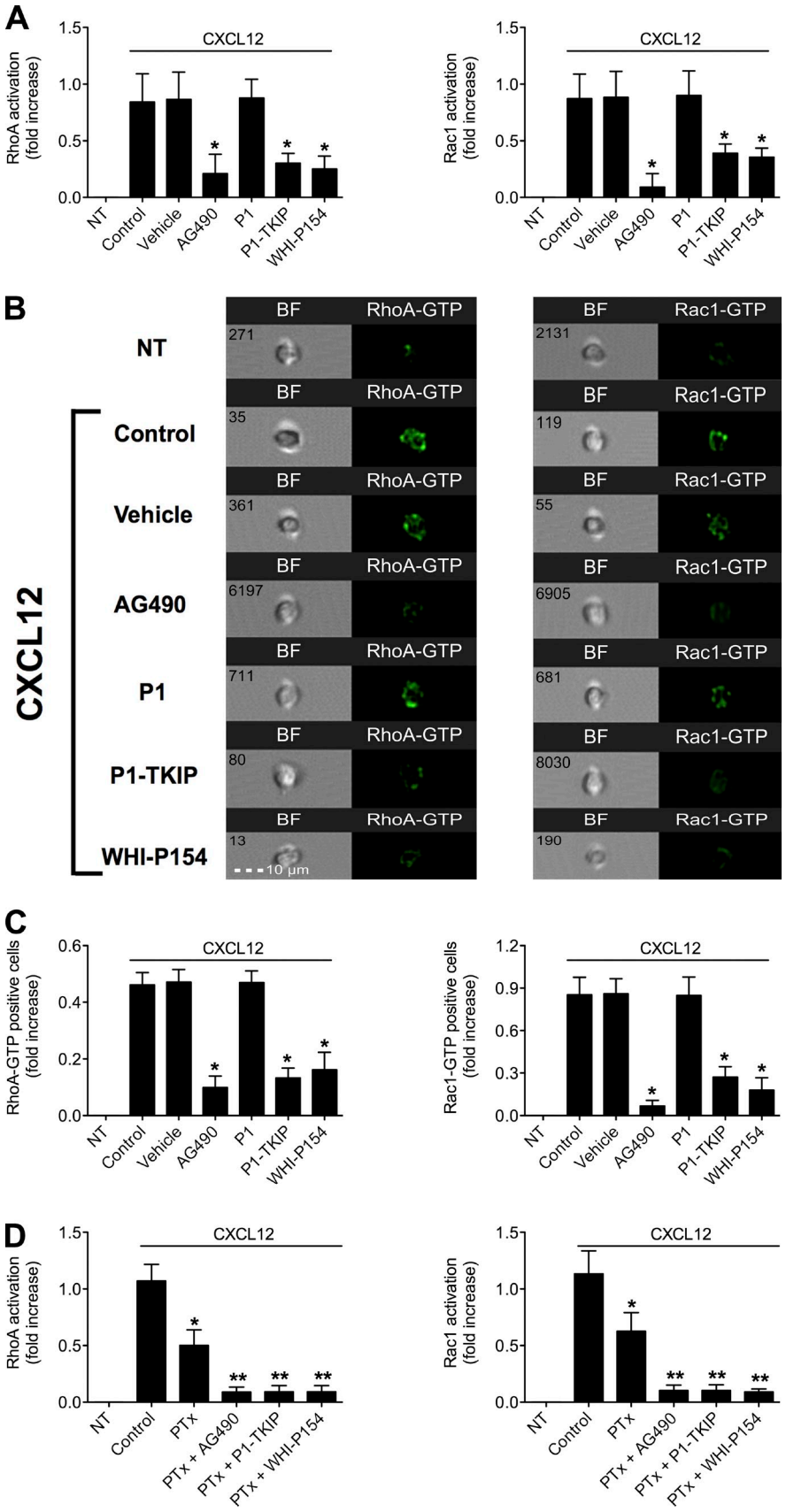

Figure 7. **JAK2 and JAK3 mediate RhoA and Rac1 activation by CXCL12.** (A) G-LISA assay detecting RhoA (left) and Rac1 (right) GTP-bound state. Lymphocytes were treated for 1 h with buffer (NT and control), DMSO (vehicle), 100 µM AG490, 40 µM Penetratin-1 (P1) or P1-TKIP, and 200 µM WHI-P154 and stimulated with 0.2 µM CXCL12. The percent fold increase of the RhoA and Rac1 activation was normalized to the level of NT intensity; mean of four experiments. *, $P < 0.01$, versus vehicle. (B) ImageStream analysis. Lymphocytes were treated and stimulated as in A; GTP-bound RhoA and Rac1 were detected with specific monoclonal antibodies (see methods) and fluorescent cells were detected and analyzed by ImageStream system IS-100. BF, bright-field channel. RhoA-GTP and Rac1-GTP are a 488-nm emission channel; representative experiment of three. Numbers identify acquired and analyzed individual cells. (C) ImageStream analysis. 5,000 cells, treated as in A and B, were analyzed. Fold increase of the RhoA-GTP (left)– and Rac1-GTP (right)–positive cells versus NT cells is shown; three experiments. *, $P < 0.01$, versus vehicle or P1. (D) G-LISA assays detecting RhoA (left) and Rac1 (right) GTP-bound state. Lymphocytes were treated with buffer (NT and control), with 2 µg/ml pertussis toxin (PTx) for 2 h, and with JAK inhibitors (100 µM AG490, 40 µM P1 or P1-TKIP, or 200 µM WHI-P154) for 1 h and then stimulated with 0.2 µM CXCL12. Fold increase of the RhoA (left) and Rac1 (right) activation was normalized to the level of NT intensity; mean of four experiments. *, $P < 0.01$, versus control; **, $P < 0.001$, versus control. Error bars show SDs.

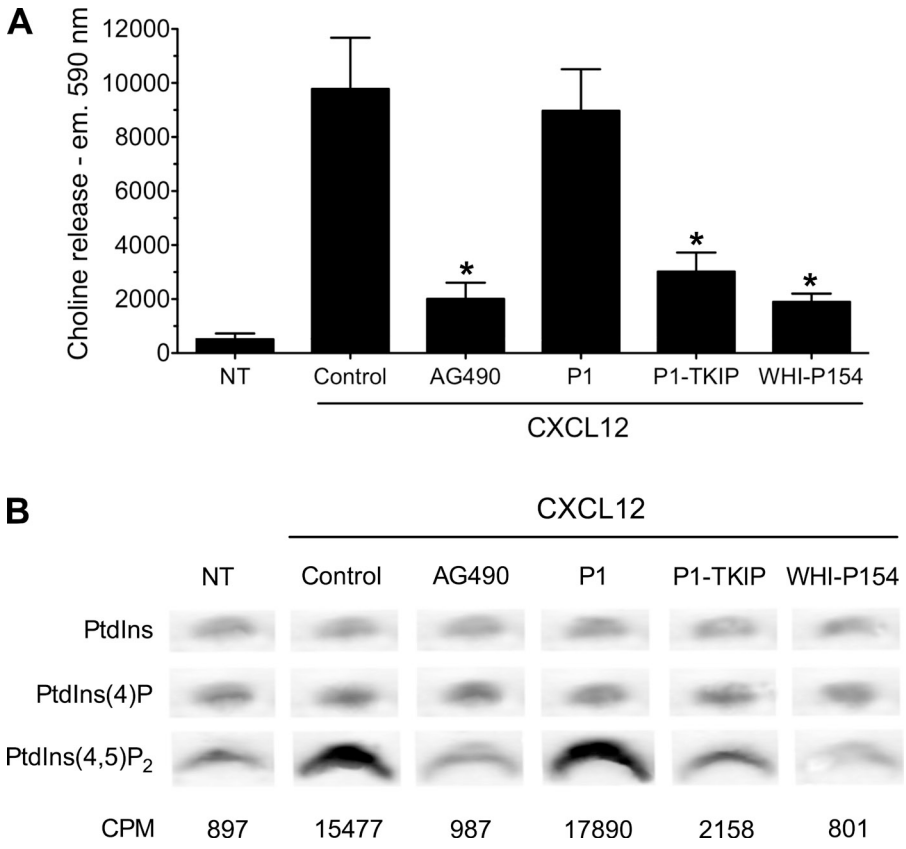

Figure 8. **JAK2 and JAK3 mediate PLD1 and PIP5K1C activation by CXCL12.** (A) Lymphocytes were treated for 1 h with buffer (NT and control), 100 µM AG490, 40 µM Penetratin-1 (P1) or P1-TKIP, or 200 µM WHI-P154 and stimulated with 0.2 µM CXCL12; mean of four experiments. Error bars show SDs. *, $P < 0.01$, versus control or P1. (B) Lymphocytes were treated as in A. Shown is an autoradiogram of ^{32}P-labeled phosphoinositides. The values (CPM) at the bottom of the figure are quantifications of incorporated radioactivity in PtdIns(4,5)P_2. Representative experiment of three.

Finally, lymphocytes displaying reduced VAV1 expression displayed defective CXCL12-triggered activation of both RhoA and Rac1 (Fig. 9, M and N). Altogether, these data strongly suggest that VAV1, upon tyrosine phosphorylation by JAKs, mediates JAK-dependent activation of the Rho module of LFA-1 affinity triggering by chemokines.

JAK2 and JAK3 mediate Rap1A activation by CXCL12

The previous data show that JAK2 and JAK3, although concurrent with PTx-sensitive heterotrimeric $G\alpha_i$ proteins, are the most critical chemokine receptor transducers controlling the activation of the Rho module of LFA-1 affinity triggering. In contrast, Rap1A activation by chemokines appears totally dependent on the transducing activity of heterotrimeric $G\alpha_i$ proteins (Fig. 1 B). However, because heterotrimeric $G\alpha_i$ proteins, JAKs, and Rho and Rap small GTPases are individually necessary, but not sufficient, to control integrin activation by chemokines, it is possible that deeper levels of integration of proadhesive signaling networks may occur. Thus, we wished to test whether JAKs could be also involved in Rap1A activation. Unexpectedly, we found that JAK inhibition by AG490 or WHI-P154 totally prevented CXCL12-triggered Rap1 activation; similar results were also obtained with the P1-TKIP peptide inhibitor (Fig. 10 A). We also confirmed these data by using JAK-specific siRNAs (Fig. S4, C and D). Thus, JAK PTKs are as critical as heterotrimeric $G\alpha_i$ proteins in controlling Rap1A activation by chemokines. These findings were surprising because activation of Rap1A in the context of chemokine-triggered integrin activation was shown to involve the Rap-specific GEF RASGRP1 (calcium DAG-GEFII; Crittenden et al., 2004; Bergmeier et al., 2007), which is not reported to be tyrosine phosphorylated nor appears regulated by tyrosine kinases. Thus, JAKs control Rap1A activation likely through different signaling mechanisms.

Rap1A is a downstream effector of RhoA and PLD1 to integrin activation by CXCL12

Previous indirect evidences suggested a possible cross talk between Rho and Rap small GTPases (Montresor et al., 2012), although a functional integration between these two signaling modules in the context of integrin activation by chemokines was never demonstrated. To address this issue, we first tested whether inhibition of Rho small GTPases could affect Rap1A activation by chemokines. To this end, we took advantage of the Trojan peptide technology, by using a P1-coupled peptide, selectively blocking RhoA (P1-RhoA-23-40; Giagulli et al., 2004) and TAT-Rac1 full-length fusion mutants (Bolomini-Vittori et al., 2009). RhoA inhibition resulted in a dose-dependent blockade of CXCL12-induced Rap1A activation, with a maximal inhibition of ~78% (Fig. 10 B). In sharp contrast, Rac1 inhibition, by using a TAT-Rac1 mutant carrying the S17N mutation (TAT-Rac1-S17N, dominant-negative mutant of Rac1) had no effect on Rap1A activation (Fig. 10 C). Wild-type TAT-Rac1 fusion protein (TAT-Rac1–wild type) and the G12V-mutated isoform (TAT-Rac1-G12V) were also ineffective (Fig. 10 C). Thus, RhoA, but not Rac1, signaling activity critically mediates CXCL12-triggered Rap1A activation.

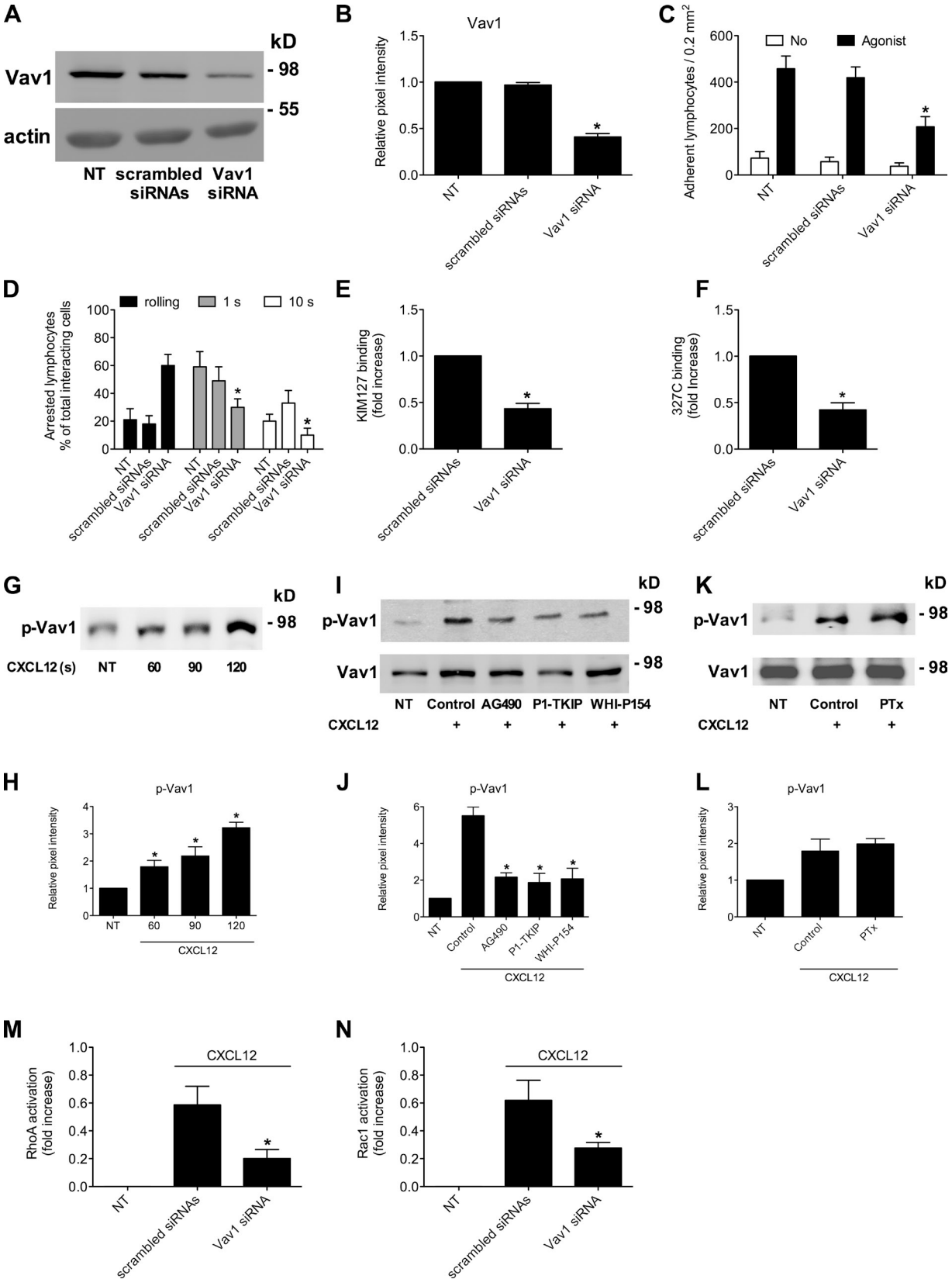

Figure 9. **VAV1 mediates JAK-dependent LFA-1 activation and RhoA and Rac1 triggering by CXCL12.** (A) Immunoblot evaluation of VAV1 expression. Lymphocytes were electroporated with a pool of four scrambled or VAV1-specific siRNAs and kept in culture for 24 h. Shown is the protein content compared with the total amount of actin. The expression level of VAV1 was assessed in whole-cell lysates with the anti-VAV1 antibody and then with the antiactin antibody for the loading control; representative experiment of four. (B) Quantification of immunoreactive bands. The relative ratio of the band intensity of total VAV1 was normalized to the level of NT intensity. Mean values of four experiments. *, $P < 0.001$, versus scrambled siRNAs. (C) Static adhesion assay to ICAM-1. Lymphocytes were treated as in A and stimulated with buffer (no) or 50 nM CXCL12 (agonist); four experiments in triplicate. *, $P < 0.01$,

We, finally, set out to define the mechanism by which RhoA controls Rap1A activation. Notably, in our context, PLD1 is downstream to RhoA activation (Bolomini-Vittori et al., 2009). Because PLD1 was suggested to control Rap1A membrane translocation (Mor et al., 2009), we tested whether PLD1 was also involved in Rap1A GDP–GTP exchange by chemokines. To examine the effect of PLD1 blockade on Rap1A activation by CXCL12, we took advantage of a previously validated P1-based peptide specifically designed to prevent PLD1 interaction with and activation by RhoA (Bolomini-Vittori et al., 2009). Pretreatment with the P1-PLD1 blocking peptide completely inhibited, in a dose-dependent manner, CXCL12-induced Rap1A activation, with a maximal inhibition of ∼91%, whereas the control P1 peptide had no effect (Fig. 10 D). Altogether, these data demonstrate that RhoA and PLD1 critically control Rap1A activation by chemokines, thus unveiling the biochemical link between JAK PTKs and Rap1A triggering by arrest chemokines.

Discussion

Leukocyte adhesion is a central homeostatic process in the immune system, and its modulation is emerging as a promising approach to treat immunity-related diseases (Ulbrich et al., 2003; Rossi and Constantin, 2008). In this study, we investigated the upstream signaling mechanisms triggered by CXCR4 and leading to LFA-1 activation in human primary T lymphocytes. Our results can be summarized as follows: (a) JAK2 and JAK3 mediate CXCL12-triggered LFA-1 affinity; (b) JAKs also mediate VLA-4 activation by CXCL12; (c) accordingly, JAKs control T lymphocyte in vivo homing to secondary lymphoid organs; (d) JAKs participate to the activation of all four proadhesive components of the Rho module of LFA-1 affinity triggering; (e) the Rho GEF VAV1 is involved in LFA-1 affinity triggering and mediates JAK-dependent activation of RhoA and Rac1 by CXCL12; (f) JAKs control Rap1A activation; and (g) activation of Rap1A by JAKs is mediated by the signaling activity of RhoA and PLD1, thus establishing Rap1A as a novel downstream effector of Rho. Overall, our data show that JAK PTKs, along with heterotrimeric $G\alpha_i$ proteins, are concurrent, necessary chemokine receptor transducers linking chemokines to the hierarchical activation of Rho and Rap signaling modules controlling integrin activation and dependent lymphocyte trafficking (Fig. S5).

At least 65 signaling molecules modulate integrin activity by chemokines, but only a few have been shown to control integrin affinity triggering by chemokines, fulfilling recently proposed criteria (Montresor et al., 2012). Accordingly, we have recently described an integrated group of signaling proteins including RhoA, Rac1, and CDC42 small GTPases, along with the two effectors PLD1 and PIP5K1C, modulating conformer-selective LFA-1 affinity triggering and homing to secondary lymphoid organs by chemokines of human primary lymphocytes (Bolomini-Vittori et al., 2009). Important questions remained open, however, such as the nature of the upstream receptor transducers leading to Rho activation and the relationships between the Rho module and other proadhesive signals activated by arrest chemokines.

Canonical signal transduction cascade triggered by chemokine receptors relies on the transducing activity of heterotrimeric $G\alpha_i$ proteins, originally implied in lymphocyte trafficking (Bargatze and Butcher, 1993). However, signaling triggered by the dissociated α_i and $\beta\gamma$ subunits appear not fully responsible for Rho activation by chemokines. Indeed, we found that PTx pretreatment only partially inhibited RhoA and Rac1 activation. Notably, the α_i subunit directly targets adenyl cyclase (Taussig et al., 1993) and SRC PTK (Ma et al., 2000), whereas the $\beta\gamma$ subunits mainly target PLC isoforms (Park et al., 1993) and PIP3K-γ (Brock et al., 2003). None of these signaling proteins can be easily related to activation of Rho GTPases in the context of LFA-1 affinity triggering by chemokines. For instance, SRC PTKs have been shown to negatively regulate LFA-1 affinity, leading to cell arrest (Giagulli et al., 2006). Moreover, the role of PIP3K in LFA-1 affinity modulation by chemokines was previously ruled out (Constantin et al., 2000). Thus, canonical signaling events triggered by heterotrimeric $G\alpha_i$ proteins, although clearly involved in regulation of integrin-mediated adhesion, seem only partially necessary but surely not sufficient to Rho activation by chemokines.

An alternative possibility was represented by JAK PTKs. Indeed, past studies suggested that JAKs can be activated by chemokines receptors (Mellado et al., 1998; Vila-Coro et al., 1999; Wong et al., 2001; Zhang et al., 2001; Soriano et al., 2003; Stein et al., 2003; Soldevila et al., 2004; García-Zepeda

versus scrambled siRNAs. (D) Underflow adhesion assays. Lymphocytes were treated as in A; three experiments. *, P < 0.01, versus scrambled siRNAs. (E and F) Lymphocytes were treated as in A and stimulated with 25 nM CXCL12. Different LFA-1 conformers were detected with the antibodies KIM127, detecting low-intermediate affinity state (E), or 327C, detecting high affinity state (F); five experiments in duplicate. *, P < 0.001, versus scrambled siRNAs. (G) Time course of VAV1 phosphorylation. Lymphocytes were treated with buffer (NT) or with 0.2 µM CXCL12 for the indicated times. Lysates were immunoprecipitated with antiphosphotyrosine antibody and probed with an anti-VAV1 antibody; representative experiment of three. (H) Quantification of immunoreactive bands. The relative ratio of the band intensity of phospho-VAV1 was normalized to the level of NT. Mean values of three experiments. *, P < 0.01, versus NT. (I) Effect of JAK inhibitors on VAV1 activation. Lymphocytes were treated with buffer (NT and control), 100 µM AG490, 40 µM P1-TKIP, or 200 µM WHI-P154 for 1 h and stimulated with 0.2 µM CXCL12 for 120 s. Lysates were immunoprecipitated and probed as in G. The expression level of total VAV1 was assessed in whole-cell lysates with the anti-VAV1 antibody; representative experiment of three. (J) Quantification of immunoreactive bands. The relative ratio of the band intensity of phospho-VAV1 was normalized to the level of NT intensity. Mean values of three experiments. *, P < 0.01, versus control. (K) VAV1 activation is independent of heterotrimeric $G\alpha_i$ proteins. Lymphocytes were treated with buffer (NT and control) or 2 µg/ml pertussis toxin (PTx) for 2 h and stimulated with 0.2 µM CXCL12 for 120 s. Lysates were immunoprecipitated as in G. The expression level of total VAV1 was assessed in whole-cell lysates with anti-VAV1 antibody; representative experiment of three. (L) Quantification of immunoreactive bands. The relative ratio of the band intensity of phospho-VAV1 was normalized to the level of NT intensity. (M and N) G-LISA assays detecting RhoA (M) and Rac1 (N) activation (GTP-bound state). Lymphocytes were treated as in A and stimulated with buffer (NT) or 0.2 µM CXCL12. Fold increase of the RhoA (M) and Rac1 (N) activation was normalized by the level of NT intensity; mean of four experiments. *, P < 0.01, versus scrambled siRNAs. Error bars show SDs.

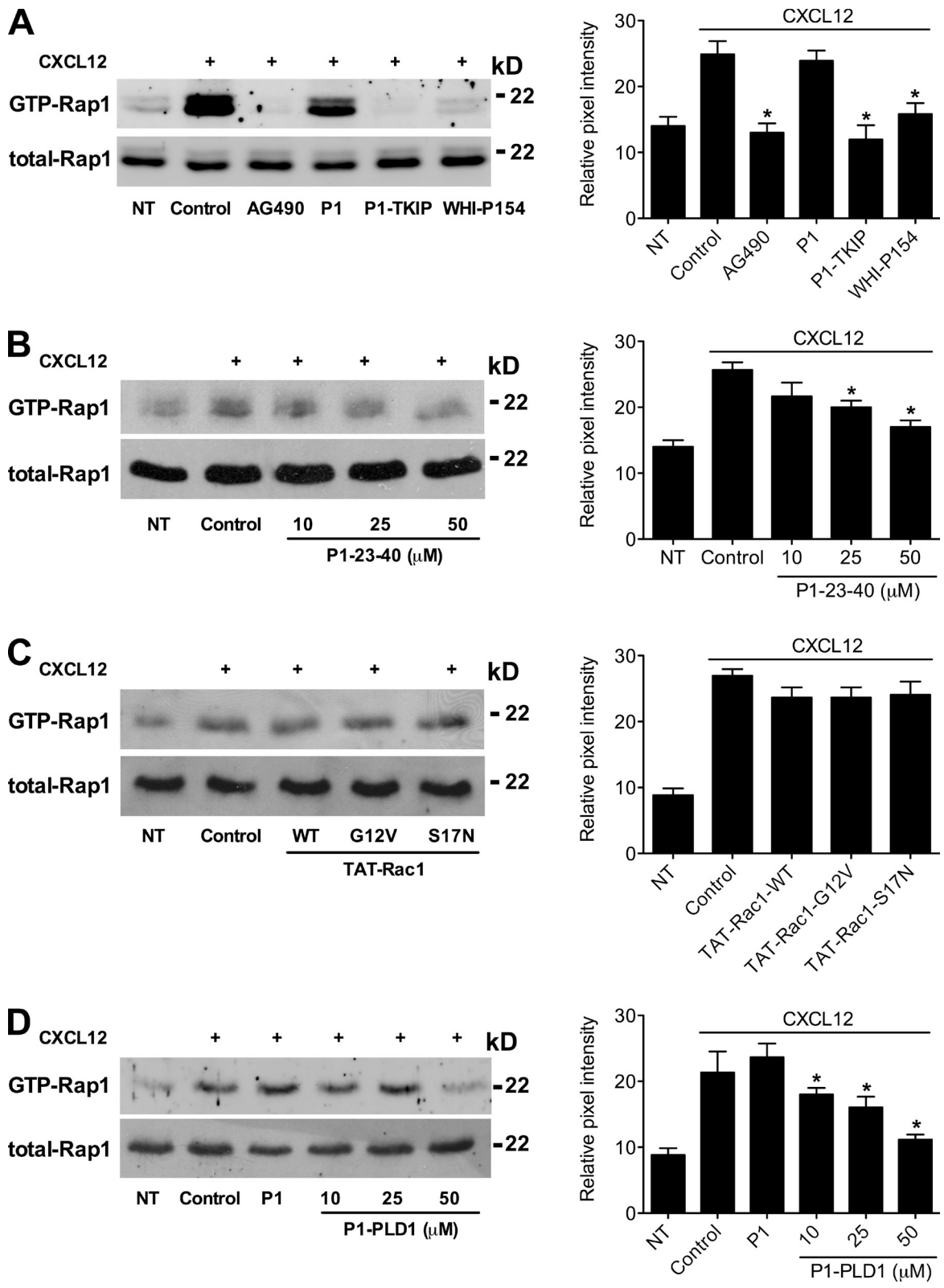

Figure 10. **JAK2, JAK3, RhoA, and PLD1 control Rap1A activation by CXCL12.** Rap1A activation was measured by pull-down assay. (A) Lymphocytes were treated for 1 h with buffer (NT and control), Penetratin-1 (P1), 100 μM AG490, 40 μM P1-TKIP, and 200 μM WHI-P154 and stimulated with 0.2 μM CXCL12; (left) representative experiment of three. (B) Lymphocytes were treated for 1 h with buffer (NT and control) or the indicated doses of P1-RhoA-23-40 (P1-23-40) and stimulated with 0.2 μM CXCL12; (left) representative experiment of five. (C) Lymphocytes were treated for 1 h with buffer (NT and control), 10 μM TAT-Rac1–wild type (WT), TAT-Rac1-G12V (G12V), and TAT-Rac1-S17N (S17N) and stimulated with 0.2 μM CXCL12; (left) representative experiment of three. (D) Lymphocytes were treated for 1 h with buffer (NT and control), P1, or indicated doses of P1-PLD1 and stimulated with 0.2 μM CXCL12; (left) representative experiment of five. (right) The relative ratio of the band intensity of GTP-Rap1A in each experiment was normalized by the level of total Rap1A intensity. Error bars show SDs. *, $P < 0.01$, versus control.

et al., 2007). We verified these findings also highlighting an isoform-selective activation of JAKs by CXCR4. Furthermore, we demonstrated that JAK2 and JAK3, the two JAK isoforms we found activated by CXCL12 in human primary T lymphocytes, mediate the activation of the Rho module of LFA-1 affinity triggering. These data demonstrate, for the first time, that JAKs are critical upstream activators of Rho small GTPases by chemokines. Notably, blockade of JAK activity by various inhibitors did not interfere with the intracellular calcium movements triggered by CXCL12 (unpublished data). Furthermore, PTx treatment did not prevent JAK activation (Fig. 2, E–H). Thus, heterotrimeric $G\alpha_i$ protein–linked and JAK-dependent pathways are concurrent, yet independent, signaling events triggered by CXCL12, even if both appear dependent on the integrity of the third intracellular loop of CXCR4 (Brelot et al., 2000; Roland et al., 2003; Ahr et al., 2005). Notably, concurrency between these signaling pathways is also supported by the combined effect of PTx and JAK inhibitor treatment on RhoA and Rac1 activation, as shown in Fig. 7 D.

Interestingly, these observations could have suggested that the activation of Rap1A, whose activation relies on the activity of the calcium-DAG–activated Rap-GEF RASGRP1, was fully dependent on heterotrimeric $G\alpha_i$ protein activity but not on JAK activity. Accordingly, we found that PTx completely blocked Rap1A activation. However, and rather surprisingly, we also discovered that inhibition of JAKs completely prevented Rap1A activation by CXCL12, showing, for the first time, an unexpected link between JAKs and Rap small GTPases. Thus, chemokine receptors, by means of two different upstream receptor transducers, activate two distinct, although cooperating, signaling modules concurrently controlling LFA-1 activation by chemokines. Importantly, this unexpected finding raised the possibility of interplay between Rho and Rap small GTPases. We verified the correctness of this hypothesis by showing that activation of Rap1A by JAKs was mediated by RhoA and by its effector PLD1. Altogether, these data highlight the complex, integrated, and hierarchical nature of the signaling machinery triggered by chemokines and controlling LFA-1 activation. Interestingly, individual blockade of heterotrimeric $G\alpha_i$ proteins, JAKs, Rap1A, RhoA, and PLD1 almost completely inhibits LFA-1 activation. Thus, each one of these signaling events, although necessary, is not sufficient. Therefore, integrin activation is controlled by an integrated macro module in which, like an engine, each part is critical but not self-sufficient to generate the final functionality (Fig. S5).

An important question concerned the link between JAKs and Rho small GTPases. Several Rho-specific GEFs have been described (Rossman et al., 2005) and few of them have been related to regulation of leukocyte adhesion, although under conditions not satisfying the aforementioned four criteria (Montresor et al., 2012). In the context of chemokine signaling leading to LFA-1 affinity regulation, an open question regards the definition of the involved Rho GEFs. We addressed this relevant issue and found that VAV1 is involved in LFA-1 affinity triggering by chemokines. Moreover, VAV1 was found tyrosine phosphorylated in a JAK-dependent manner. Because tyrosine phosphorylation is a major mechanism of activation of VAV1 (Aghazadeh et al., 2000), these data suggest that VAV1 links JAKs to Rho module activation by chemokines. Notably, our data show a consistent, but still not complete, inhibition of LFA-1, RhoA, and Rac1 activation by VAV1 siRNAs. This suggests that JAKs may phosphorylate and activate other Rho GEFs involved in signaling mechanisms regulating LFA-1 activation. This interesting possibility may lead to a deeper characterization of the Rho module of LFA-1 affinity triggering and will be matter for future investigations.

RhoA-activated PLD1 appears to be the intersection point between Rho and Rap signaling. Indeed, we showed that PLD1 inhibition prevents Rap1A activation. Interestingly, Rac1 blockade did not affect Rap1A activation by CXCL12. This is likely in keeping with a preponderant role of RhoA in PLD1 activation (Bolomini-Vittori et al., 2009). Because PLD1 does not have Rap1A GEF activity, we hypothesize, in agreement with previous data (Mor et al., 2009), that PLD1 could control Rap1A translocation to specific, still unidentified, membrane compartments involved in LFA-1 affinity regulation, allowing Rap1A to interact with Rap GEFs, such as RASGRP1, and, thus, activating GDP–GTP exchange (Fig. S5). Notably, the complexity and rapidness of the signaling machinery controlling integrin activation by chemokines may suggest the occurrence of preassembled modules on plasma membrane domains, such as rafts or microvilli, ready to be activated in a fraction of seconds upon translocation of critical components.

The Rho module of LFA-1 affinity triggering, although validated in human primary T and B lymphocytes, was shown not to be a universal mechanism of integrin activation. For instance, CXCL9-triggered adhesion on ICAM-1, which does not rely on LFA-1 affinity triggering, was also shown to be independent of RhoA (Pasvolsky et al., 2008), although JAKs are activated by CXCL9 (Fig. S3). Moreover, in neoplastic B lymphocytes isolated from chronic lymphocytic leukemia patients, we found that the regulatory role of Rac1, CDC42, and PIP5K1C displays disease- and patient-specific variability (Montresor et al., 2009). In contrast, RhoA and PLD1 appear always critical. Thus, it will be of great interest to examine the involvement of JAK PTKs and of the other components of the Rap–Rho macro module of integrin activation under different conditions, including different agonists and cellular contexts, and test whether the functional relationships between Rho and Rap are conserved.

Materials and methods

Human primary cells and reagents

Informed consent to this work was provided by the University of Verona; the University of Verona Ethics Committee approved experimentation with human primary cells. Human primary T lymphocytes were isolated from the whole blood of healthy donors by Ficoll and Percoll gradient sedimentation. Purity of T lymphocyte preparation was evaluated by flow cytometry after staining with FITC-conjugated anti-CD3 antibody and was >95%. Isolated T lymphocytes were kept at 37°C in standard adhesion buffer (PBS, 1 mM $CaCl_2$, 1 mM $MgCl_2$, and 10% FBS, pH 7.2) and used within 1 h. FBS was obtained from Lonza. Human CXCL12, human CXCL9, mouse CCL21, ICAM-1, VCAM-1, and E-selectin were obtained from R&D Systems. FITC-conjugated goat antibody to mouse was purchased from Sigma-Aldrich. Monoclonal anti–LFA-1 was purchased from ATCC (KIM127) or provided by K. Kikly (Eli Lilly and Co., Indianapolis, IN; 327C and 327A).

Mouse monoclonal antiactive RhoA (26904) and antiactive Rac1 (26903) antibodies were obtained from NewEast Biosciences. Immobilized phosphotyrosine monoclonal mouse antibody (P-Tyr-100), rabbit monoclonal anti-JAK2 (D2E12), rabbit polyclonal anti-JAK3, and rabbit polyclonal anti-VAV1 antibodies were obtained from Cell Signaling Technology. 1-mm-diameter glass capillary tubes were purchased from Drummond Scientific Company. Tyrphostin AG490 was obtained from Sigma-Aldrich. WHI-P154 was obtained from EMD Millipore. PTx was obtained from Tocris Bioscience. [^{32}P]PO_4 was purchased from GE Healthcare. siRNAs (ON-TARGETplus SMARTpool) were obtained from Thermo Fisher Scientific (JAK2 a, 5′-CGAAUAAGGUACAGAUUUC-3′; b, 5′-UUACAGAGGCCUACUCAUA-3′; c, 5′-AAUCAAACCUUCUAGUCUU-3′; and d, 5′-GGAAUGGCCUGCCUUACGA-3′; and JAK3 a, 5′-CCUCAUCUCUUCAGACUAU-3′; b, 5′-GCAGACACUUAGCUUGGAA-3′; c, 5′-CGUCCUGGCUCCUAUGUUC-3′; and d, 5′-UGUACGAGCUCUUCACCUA-3′). VAV1 was 5′-CGUCGAGGUCAAGCACAUUdTdT-3′, as reported in García-Bernal et al. (2005).

Trojan nanovector technology

The control P1 and the JAK2-blocking (P1-TKIP) peptides were synthesized by GenScript. The P1-TKIP peptide (RQIKIWFQNRRMKWKKGWLVFFVIFYFFR; underlined letter highlights the important inserted glycine allowing flexibility of the fusion peptide) encompassed the complete P1 sequence (16 aa), an inserted glycine to allow flexibility of the fusion peptide, and the TKIP sequence (12 aa) blocking specifically JAK2 autophosphorylation (Flowers et al., 2004). The P1-TKIP peptide displayed the following properties: 29 aa, molecular weight of 3969.89, and P_i of 12.02. 10-mM stock solutions in DMSO were kept at −20°C and diluted in adhesion buffer immediately before the experiments. Standard treatment of cells with peptides was for 1 h at 37°C in 24- or 6-well plates.

Immunoprecipitation and Western blot

Cells were treated as indicated, stimulated with 0.2 µM CXCL12, and then lysed in ice-cold 1% NP-40 buffer, containing phosphatase inhibitors and complete protease inhibitor cocktail (Roche). Lysates were quantified by Bradford assay (Bio-Rad Laboratories), and equal amounts of proteins were subjected to 10% SDS-PAGE, or phosphotyrosine was enriched by immobilized phosphotyrosine monoclonal mouse antibody (P-Tyr-100) immunoprecipitation and blotted. After incubation with anti-JAK2, anti-JAK3, or anti-VAV1 primary antibodies and HRP-coupled secondary antibodies (GE Healthcare), immunoreactive bands were visualized by ECL detection (EMD Millipore). Intensities of band signals were quantified by densitometric analysis (Quantity One; Bio-Rad Laboratories).

Static adhesion assay

Human primary T lymphocytes were suspended at 5 × 10^6/ml in standard adhesion buffer. Adhesion assays were performed on 18-well glass slides coated with human ICAM-1 at 1 µg/ml in PBS; 20 µl of cell suspension was added to the wells and stimulated for 1 min at 37°C with 5 µl CXCL12 at a 0.2-µM final concentration. After rapid washing, adherent cells were fixed in ice-cold 1.5% glutaraldehyde in PBS, and still images of adherent cells in 0.2-mm^2 fields were acquired at 20× phase contrast magnification, NA 0.40, with a charge-coupled device camera (ICD-42B; Ikegami) connected to an inverted microscope (IX50; Olympus). Image acquisition and computer-assisted enumeration of adherent cells were performed with ImageJ (National Institutes of Health).

Underflow adhesion assay

Human primary T lymphocytes were suspended at 10^6/ml in standard adhesion. Cell behavior underflow at wall shear stress of 2 dyne/cm^2 was studied with the BioFlux 200 system (Fluxion Biosciences). 48-well plate microfluidics were first co-coated overnight at room temperature with 2.5 µg/ml human E-selectin and 5 µg/ml human ICAM-1 in PBS. Immediately before use, microfluidic channels were washed with PBS and then coated with 2 µM CXCL12 in PBS for 3 h at room temperature. After washing of microfluidics with adhesion buffer, the behavior of interacting lymphocytes was digitally recorded (25 frames/s). 0.2-mm^2 single areas were recorded for ≥120 s. Interactions of 40 ms or longer were considered significant and scored. Lymphocytes that remained firmly adherent for ≥1 s were considered fully arrested. Cells arrested for ≥1 s and then detached, or for 10 s and then remained adherent, were scored separately and plotted as independent groups. Video acquisition was performed with a digital recorder (DN-400 DV-HDV; Datavideo) at 20× phase contrast magnification (NA 0.40) with a charge-coupled device camera (ICD-42B) connected to an inverted microscope (IX50). Computer-assisted frame-by-frame analysis of cell behavior was performed with ImageJ.

Intravital microscopy

In vivo lymphocyte arrest on blood vessel endothelial cells was studied in secondary lymphoid organs by intravital microscopy analysis (Bolomini-Vittori et al., 2009). In brief, lymphocytes (20 × 10^6/ml in DMEM without sodium bicarbonate supplemented with 20 mM Hepes and 5% FBS, pH 7.2) were labeled with either CMFDA (1 min at 37°C) or CMTMR (3 min at 37°C). 20 × 10^6 labeled cells were injected i.v. in the tail vein of C57BL/6J mice. In situ video microscopic analyses were performed in HEVs in an exteriorized Peyer's patch. Experiments were recorded at 20× magnification, NA 0.40, on a digital recorder (DN-400 DV-HDV) with a highly sensitive fast video camera (25 frames/s, capable of 1/2 subframe with 20-ms recording; Silicon Intensified Target; DAGE-MTI) connected to a microscope (BX50WI; Olympus) and analyzed subframe by subframe. Computer-assisted frame-by-frame analysis of cell behavior was performed with ImageJ. Cell behavior was analyzed over a period of 20–30 min starting at 2 min after i.v. injection. Interactions of >20 ms were considered significant and were scored. Cells were considered to be interacting whether they rolled, arrested, or both. Lymphocytes that remained firmly adherent on the venular wall for ≥1 s were considered fully arrested. Cells that arrested for ≥1 s and then detached or for 10 s and remained adherent were scored separately and plotted as independent groups.

Measurement of LFA-1 affinity states

Lymphocytes suspended in standard adhesion buffer at 2 × 10^6/ml were stimulated for 10 s with 0.2 µM CXCL12 under stirring at 37°C in the presence of 10 µg/ml KIM127 (reporter for extended conformation epitope possibly corresponding to a low or intermediate affinity state; Robinson et al., 1992; Shimaoka et al., 2006; Stanley et al., 2008) or 327C (reporter for extended conformation epitope related to a high affinity state; Lum et al., 2002). After rapid washing, the cells were stained with FITC-conjugated secondary antibody and analyzed by cytofluorimetric quantification.

siRNA technique

Lymphocytes were plated at 5 × 10^6/ml in RPMI 1640 + 2 mM glutamine + 10% FBS for 2 h before silencing. Cells, suspended in nucleofector buffer at 5 × 10^7/ml, were electroporated with Nucleofector (Amaxa Biosystems) in the presence of 3 µg of specific siRNA according to the manufacturer's instructions (Thermo Fisher Scientific). The efficiency of siRNA nucleoporation was evaluated with FITC-conjugated siRNA, and the efficacy of gene silencing was evaluated by Western blotting.

RhoA and Rac1 activation assays

RhoA and Rac1 activations were determined using an activation assay kit (G-LISA; Cytoskeleton, Inc.), by adaption of the protocols as previously reported (Bolomini-Vittori et al., 2009). In brief, lymphocytes were treated as indicated and then stimulated with 0.2 µM CXCL12 and lysed, following the manufacturer's protocol, and levels of GTP-bound RhoA and Rac1 were measured (absorbance at 490 nm) by a plate reader (VICTOR X5 Multilabel Plate Reader; PerkinElmer).

ImageStream analysis

Cells suspended at 20 × 10^6/ml in standard adhesion buffer were treated with JAK inhibitors and then stimulated with 0.2 µM CXCL12. After washing, cells were fixed in ice-cold 4% formaldehyde and stained in permeabilization buffer (PBS, 0.5% saponin, 4 mM azide, and 10% FBS), containing antiactive RhoA or antiactive Rac1 antibodies. After incubation with FITC-conjugated secondary antibody in permeabilization buffer, fluorescent cells were analyzed with a flow cytometer (ImageStream IS-100; EMD Millipore) improved with extended depth of field technology upon acquisition at 40× magnification, NA 0.75, with the INSPIRE software v. 3.0 (EMD Millipore). Bright-field illumination is provided by a white light (halogen) lamp, and fluorescence excitation is achieved with a solid-state 488-nm laser (40-mW power). Single cell analysis was performed with the IDEAS software v. 4.0 (EMD Millipore).

Rap1 activation assay

Rap1 activation was performed by pull-down assay with RalGDS–Rap-binding domain following the manufacturer's instructions (Rap1 activation assay kit; EMD Millipore). Cells were treated as indicated and stimulated with 0.2 µM CXCL12, and cell lysates were separated by electrophoresis and blotted onto nitrocellulose (GE Healthcare). After incubation with anti-Rap1 primary antibody and HRP-coupled secondary antibodies (GE Healthcare), immunoreactive bands were visualized by ECL (EMD Millipore). Intensities of band signals were quantified by using the densitometric software Quantity One.

PLD1 activation assay

Activation of phosphatidylcholine-specific PLD1 was evaluated by measuring choline release with the PLD assay kit (Cayman Chemical; Bolomini-Vittori et al., 2009). In brief, cells were treated as indicated, stimulated with 0.2 µM CXCL12, and then lysed immediately after the stimulation. Cell lysates were centrifuged at 10,000 *g* for 15 min, and the supernatants were processed following the manufacturer's instructions. Fluorescence was detected by a plate reader with 530–540-nm excitation and 590-nm emission (VICTOR X5 Multilabel Plate Reader).

PIP5K1C activation assay

PIP5K1C activity was evaluated by measuring the accumulation of PtdIns(4,5)P_2, as previously reported (Bolomini-Vittori et al., 2009). Human primary T lymphocytes, suspended at 30 × 10^6/ml in Hanks' buffer, pH 7.4, and 1 mg/ml D-glucose, were labeled for 3 h at 37°C with 300 µCi [^{32}P]PO_4. After stimulation with 0.2 µM CXCL12, 0.8 ml of cell suspension (24 × 10^6 cells) was directly lysed in 3 ml of methanol/chloroform 2:1. The chloroform phase was extracted, N_2 stream was evaporated, and the remaining lipid pellet was dissolved in 50 µl methanol/chloroform 2:1. Radioactive samples were spotted on thin-layer chromatography plates (Silica Gel 60), impregnated with 1.2% potassium oxalate, and preactivated at 70°C, and then chromatographed in chloroform/methanol/2.5 N ammonium hydroxide (9:7:2 vol/vol). The ^{32}P-labeled products, identified by comparison with standards, were visualized by autoradiography. Radioactivity was quantified with Instant Imager (Packard).

Statistical analysis

Statistical analysis was performed by calculating the mean and standard deviation from different experiments. Significance was calculated by analysis of variance followed by Dunnett's post hoc test versus the control condition indicated in each graph.

Online supplemental material

Fig. S1 shows rapid static adhesion and LFA-1 affinity increase induced by mouse CCL21. Fig. S2 shows the effects of JAK PTK inhibitors and knockdown by siRNAs in static and underflow adhesion assays on VCAM-1. Fig. S3 shows JAK2 and JAK3 phosphorylation triggered by CXCL9. Fig. S4 shows the effects of JAK PTK knockdown by siRNAs on RhoA, Rac1, and Rap1 activations. Fig. S5 shows a model of LFA-1 activation by chemokines based on the described findings. Online supplemental material is available at http://www.jcb.org/cgi/content/full/jcb.201303067/DC1.

We are grateful to Dr. Kristine Kikly (Eli Lilly and Co.) for providing the anti–LFA-1 mAbs 327C and A. We thank the Centro Grandi Attrezzature of the University of Verona for providing the ImageStream facility.

This work was supported by the Italian Association for Cancer Research (IG 8690 to C. Laudanna), Ministero dell'Istruzione, dell'Università e della Ricerca (PRIN 2009), Fondazione Cariverona, nanomedicine project of the University of Verona and Fondazione Cariverona (C. Laudanna and G. Constantin), European Research Council (grant 261079 NEUROTRAFFICKING to G. Constantin), the National Multiple Sclerosis Society (New York, NY; to G. Constantin), and Fondazione Italiana Sclerosi Multipla (to G. Constantin).

The authors have no conflicting financial interests.

Submitted: 13 March 2013
Accepted: 13 November 2013

References

Aghazadeh, B., W.E. Lowry, X.Y. Huang, and M.K. Rosen. 2000. Structural basis for relief of autoinhibition of the Dbl homology domain of proto-oncogene Vav by tyrosine phosphorylation. *Cell*. 102:625–633. http://dx.doi.org/10.1016/S0092-8674(00)00085-4

Ahr, B., M. Denizot, V. Robert-Hebmann, A. Brelot, and M. Biard-Piechaczyk. 2005. Identification of the cytoplasmic domains of CXCR4 involved in Jak2 and STAT3 phosphorylation. *J. Biol. Chem.* 280:6692–6700. http://dx.doi.org/10.1074/jbc.M408481200

Bargatze, R.F., and E.C. Butcher. 1993. Rapid G protein-regulated activation event involved in lymphocyte binding to high endothelial venules. *J. Exp. Med.* 178:367–372. http://dx.doi.org/10.1084/jem.178.1.367

Battistini, L., L. Piccio, B. Rossi, S. Bach, S. Galgani, C. Gasperini, L. Ottoboni, D. Ciabini, M.D. Caramia, G. Bernardi, et al. 2003. CD8+ T cells from patients with acute multiple sclerosis display selective increase of adhesiveness in brain venules: a critical role for P-selectin glycoprotein ligand-1. *Blood*. 101:4775–4782. http://dx.doi.org/10.1182/blood-2002-10-3309

Bergmeier, W., T. Goerge, H.W. Wang, J.R. Crittenden, A.C. Baldwin, S.M. Cifuni, D.E. Housman, A.M. Graybiel, and D.D. Wagner. 2007. Mice lacking the signaling molecule CalDAG-GEFI represent a model for leukocyte adhesion deficiency type III. *J. Clin. Invest.* 117:1699–1707. http://dx.doi.org/10.1172/JCI30575

Bolomini-Vittori, M., A. Montresor, C. Giagulli, D. Staunton, B. Rossi, M. Martinello, G. Constantin, and C. Laudanna. 2009. Regulation of conformer-specific activation of the integrin LFA-1 by a chemokine-triggered Rho signaling module. *Nat. Immunol.* 10:185–194. http://dx.doi.org/10.1038/ni.1691

Brelot, A., N. Heveker, M. Montes, and M. Alizon. 2000. Identification of residues of CXCR4 critical for human immunodeficiency virus coreceptor and chemokine receptor activities. *J. Biol. Chem.* 275:23736–23744. http://dx.doi.org/10.1074/jbc.M000776200

Brock, C., M. Schaefer, H.P. Reusch, C. Czupalla, M. Michalke, K. Spicher, G. Schultz, and B. Nürnberg. 2003. Roles of Gβγ in membrane recruitment and activation of p110γ/p101 phosphoinositide 3-kinase γ. *J. Cell Biol.* 160:89–99. http://dx.doi.org/10.1083/jcb.200210115

Cockcroft, S., G.M. Thomas, A. Fensome, B. Geny, E. Cunningham, I. Gout, I. Hiles, N.F. Totty, O. Truong, and J.J. Hsuan. 1994. Phospholipase D: a downstream effector of ARF in granulocytes. *Science*. 263:523–526. http://dx.doi.org/10.1126/science.8290961

Constantin, G., M. Majeed, C. Giagulli, L. Piccio, J.Y. Kim, E.C. Butcher, and C. Laudanna. 2000. Chemokines trigger immediate beta2 integrin affinity and mobility changes: differential regulation and roles in lymphocyte arrest under flow. *Immunity*. 13:759–769. http://dx.doi.org/10.1016/S1074-7613(00)00074-1

Crittenden, J.R., W. Bergmeier, Y. Zhang, C.L. Piffath, Y. Liang, D.D. Wagner, D.E. Housman, and A.M. Graybiel. 2004. CalDAG-GEFI integrates signaling for platelet aggregation and thrombus formation. *Nat. Med.* 10:982–986. http://dx.doi.org/10.1038/nm1098

Feng, J., B.A. Witthuhn, T. Matsuda, F. Kohlhuber, I.M. Kerr, and J.N. Ihle. 1997. Activation of Jak2 catalytic activity requires phosphorylation of Y1007 in the kinase activation loop. *Mol. Cell. Biol.* 17:2497–2501.

Flowers, L.O., H.M. Johnson, M.G. Mujtaba, M.R. Ellis, S.M. Haider, and P.S. Subramaniam. 2004. Characterization of a peptide inhibitor of Janus kinase 2 that mimics suppressor of cytokine signaling 1 function. *J. Immunol.* 172:7510–7518.

García-Bernal, D., N. Wright, E. Sotillo-Mallo, C. Nombela-Arrieta, J.V. Stein, X.R. Bustelo, and J. Teixidó. 2005. Vav1 and Rac control chemokine-promoted T lymphocyte adhesion mediated by the integrin alpha4beta1. *Mol. Biol. Cell*. 16:3223–3235. http://dx.doi.org/10.1091/mbc.E04-12-1049

García-Zepeda, E.A., I. Licona-Limón, M.F. Jiménez-Sólomon, and G. Soldevila. 2007. Janus kinase 3-deficient T lymphocytes have an intrinsic defect in CCR7-mediated homing to peripheral lymphoid organs. *Immunology*. 122:247–260. http://dx.doi.org/10.1111/j.1365-2567.2007.02634.x

Giagulli, C., E. Scarpini, L. Ottoboni, S. Narumiya, E.C. Butcher, G. Constantin, and C. Laudanna. 2004. RhoA and zeta PKC control distinct modalities of LFA-1 activation by chemokines: critical role of LFA-1 affinity triggering in lymphocyte in vivo homing. *Immunity*. 20:25–35. http://dx.doi.org/10.1016/S1074-7613(03)00350-9

Giagulli, C., L. Ottoboni, E. Caveggion, B. Rossi, C. Lowell, G. Constantin, C. Laudanna, and G. Berton. 2006. The Src family kinases Hck and Fgr are dispensable for inside-out, chemoattractant-induced signaling regulating beta 2 integrin affinity and valency in neutrophils, but are required for beta 2 integrin-mediated outside-in signaling involved in sustained adhesion. *J. Immunol.* 177:604–611.

Jarquin-Pardo, M., A. Fitzpatrick, F.J. Galiano, E.A. First, and J.N. Davis. 2007. Phosphatidic acid regulates the affinity of the murine phosphatidylinositol 4-phosphate 5-kinase-Ibeta for phosphatidylinositol-4-phosphate. *J. Cell. Biochem.* 100:112–128. http://dx.doi.org/10.1002/jcb.21027

Kim, M., C.V. Carman, W. Yang, A. Salas, and T.A. Springer. 2004. The primacy of affinity over clustering in regulation of adhesiveness of the integrin $\alpha_L\beta_2$. *J. Cell Biol.* 167:1241–1253. http://dx.doi.org/10.1083/jcb.200404160

Krauss, M., M. Kinuta, M.R. Wenk, P. De Camilli, K. Takei, and V. Haucke. 2003. ARF6 stimulates clathrin/AP-2 recruitment to synaptic membranes by activating phosphatidylinositol phosphate kinase type Iγ. *J. Cell Biol.* 162:113–124. http://dx.doi.org/10.1083/jcb.200301006

Ley, K., C. Laudanna, M.I. Cybulsky, and S. Nourshargh. 2007. Getting to the site of inflammation: the leukocyte adhesion cascade updated. *Nat. Rev. Immunol.* 7:678–689. http://dx.doi.org/10.1038/nri2156

Lum, A.F., C.E. Green, G.R. Lee, D.E. Staunton, and S.I. Simon. 2002. Dynamic regulation of LFA-1 activation and neutrophil arrest on intercellular adhesion molecule 1 (ICAM-1) in shear flow. *J. Biol. Chem.* 277:20660–20670. http://dx.doi.org/10.1074/jbc.M202223200

Luo, B.H., C.V. Carman, and T.A. Springer. 2007. Structural basis of integrin regulation and signaling. *Annu. Rev. Immunol.* 25:619–647. http://dx.doi.org/10.1146/annurev.immunol.25.022106.141618

Ma, Y.C., J. Huang, S. Ali, W. Lowry, and X.Y. Huang. 2000. Src tyrosine kinase is a novel direct effector of G proteins. *Cell*. 102:635–646. http://dx.doi.org/10.1016/S0092-8674(00)00086-6

Matsuda, T., J. Feng, B.A. Witthuhn, Y. Sekine, and J.N. Ihle. 2004. Determination of the transphosphorylation sites of Jak2 kinase. *Biochem. Biophys. Res. Commun.* 325:586–594. http://dx.doi.org/10.1016/j.bbrc.2004.10.071

Mellado, M., J.M. Rodríguez-Frade, A. Aragay, G. del Real, A.M. Martín, A.J. Vila-Coro, A. Serrano, F. Mayor Jr., and C. Martínez-A. 1998. The chemokine monocyte chemotactic protein 1 triggers Janus kinase 2 activation and tyrosine phosphorylation of the CCR2B receptor. *J. Immunol.* 161:805–813.

Montresor, A., M. Bolomini-Vittori, S.I. Simon, A. Rigo, F. Vinante, and C. Laudanna. 2009. Comparative analysis of normal versus CLL B-lymphocytes reveals patient-specific variability in signaling mechanisms controlling LFA-1 activation by chemokines. *Cancer Res.* 69:9281–9290. http://dx.doi.org/10.1158/0008-5472.CAN-09-2009

Montresor, A., L. Toffali, G. Constantin, and C. Laudanna. 2012. Chemokines and the signaling modules regulating integrin affinity. *Front Immunol*. 3:127. http://dx.doi.org/10.3389/fimmu.2012.00127

Mor, A., J.P. Wynne, I.M. Ahearn, M.L. Dustin, G. Du, and M.R. Philips. 2009. Phospholipase D1 regulates lymphocyte adhesion via upregulation of Rap1 at the plasma membrane. *Mol. Cell. Biol.* 29:3297–3306. http://dx.doi.org/10.1128/MCB.00366-09

Oh, D.Y., S.Y. Park, J.H. Cho, K.S. Lee, S. Min, and J.S. Han. 2007. Phospholipase D1 activation through Src and Ras is involved in basic fibroblast growth factor-induced neurite outgrowth of H19-7 cells. *J. Cell. Biochem.* 101:221–234. http://dx.doi.org/10.1002/jcb.21166

Park, D., D.Y. Jhon, C.W. Lee, K.H. Lee, and S.G. Rhee. 1993. Activation of phospholipase C isozymes by G protein beta gamma subunits. *J. Biol. Chem.* 268:4573–4576.

Pasvolsky, R., V. Grabovsky, C. Giagulli, Z. Shulman, R. Shamri, S.W. Feigelson, C. Laudanna, and R. Alon. 2008. RhoA is involved in LFA-1 extension triggered by CXCL12 but not in a novel outside-in LFA-1 activation facilitated by CXCL9. *J. Immunol.* 180:2815–2823.

Piccio, L., B. Rossi, L. Colantonio, R. Grenningloh, A. Gho, L. Ottoboni, J.W. Homeister, E. Scarpini, M. Martinello, C. Laudanna, et al. 2005. Efficient recruitment of lymphocytes in inflamed brain venules requires expression of cutaneous lymphocyte antigen and fucosyltransferase-VII. *J. Immunol.* 174:5805–5813.

Robinson, M.K., D. Andrew, H. Rosen, D. Brown, S. Ortlepp, P. Stephens, and E.C. Butcher. 1992. Antibody against the Leu-CAM beta-chain (CD18) promotes both LFA-1- and CR3-dependent adhesion events. *J. Immunol.* 148:1080–1085.

Roland, J., B.J. Murphy, B. Ahr, V. Robert-Hebmann, V. Delauzun, K.E. Nye, C. Devaux, and M. Biard-Piechaczyk. 2003. Role of the intracellular domains of CXCR4 in SDF-1-mediated signaling. *Blood*. 101:399–406. http://dx.doi.org/10.1182/blood-2002-03-0978

Rossi, B., and G. Constantin. 2008. Anti-selectin therapy for the treatment of inflammatory diseases. *Inflamm. Allergy Drug Targets*. 7:85–93. http://dx.doi.org/10.2174/187152808785107633

Rossman, K.L., C.J. Der, and J. Sondek. 2005. GEF means go: turning on RHO GTPases with guanine nucleotide-exchange factors. *Nat. Rev. Mol. Cell Biol.* 6:167–180. http://dx.doi.org/10.1038/nrm1587

Shimaoka, M., M. Kim, E.H. Cohen, W. Yang, N. Astrof, D. Peer, A. Salas, A. Ferrand, and T.A. Springer. 2006. AL-57, a ligand-mimetic antibody to integrin LFA-1, reveals chemokine-induced affinity up-regulation in lymphocytes. *Proc. Natl. Acad. Sci. USA*. 103:13991–13996. http://dx.doi.org/10.1073/pnas.0605716103

Siddiqi, A.R., G.E. Srajer, and C.C. Leslie. 2000. Regulation of human PLD1 and PLD2 by calcium and protein kinase C. *Biochim. Biophys. Acta*. 1497:103–114. http://dx.doi.org/10.1016/S0167-4889(00)00049-5

Soldevila, G., I. Licona, A. Salgado, M. Ramírez, R. Chávez, and E. García-Zepeda. 2004. Impaired chemokine-induced migration during T-cell development in the absence of Jak 3. *Immunology*. 112:191–200. http://dx.doi.org/10.1111/j.1365-2567.2004.01863.x

Soriano, S.F., A. Serrano, P. Hernanz-Falcón, A. Martín de Ana, M. Monterrubio, C. Martínez, J.M. Rodríguez-Frade, and M. Mellado. 2003. Chemokines integrate JAK/STAT and G-protein pathways during chemotaxis and calcium flux responses. *Eur. J. Immunol.* 33:1328–1333. http://dx.doi.org/10.1002/eji.200323897

Stanley, P., A. Smith, A. McDowall, A. Nicol, D. Zicha, and N. Hogg. 2008. Intermediate-affinity LFA-1 binds alpha-actinin-1 to control migration at the leading edge of the T cell. *EMBO J.* 27:62–75. http://dx.doi.org/10.1038/sj.emboj.7601959

Stein, J.V., S.F. Soriano, C. M'rini, C. Nombela-Arrieta, G.G. de Buitrago, J.M. Rodríguez-Frade, M. Mellado, J.P. Girard, and C. Martínez-A. 2003. CCR7-mediated physiological lymphocyte homing involves activation of a tyrosine kinase pathway. *Blood*. 101:38–44. http://dx.doi.org/10.1182/blood-2002-03-0841

Sun, Y., Y. Fang, M.S. Yoon, C. Zhang, M. Roccio, F.J. Zwartkruis, M. Armstrong, H.A. Brown, and J. Chen. 2008. Phospholipase D1 is an effector of Rheb in the mTOR pathway. *Proc. Natl. Acad. Sci. USA*. 105:8286–8291. http://dx.doi.org/10.1073/pnas.0712268105

Taussig, R., J.A. Iñiguez-Lluhi, and A.G. Gilman. 1993. Inhibition of adenylyl cyclase by Gi alpha. *Science*. 261:218–221. http://dx.doi.org/10.1126/science.8327893

Ulbrich, H., E.E. Eriksson, and L. Lindbom. 2003. Leukocyte and endothelial cell adhesion molecules as targets for therapeutic interventions in inflammatory disease. *Trends Pharmacol. Sci.* 24:640–647. http://dx.doi.org/10.1016/j.tips.2003.10.004

Vila-Coro, A.J., J.M. Rodríguez-Frade, A. Martín De Ana, M.C. Moreno-Ortíz, C. Martínez-A, and M. Mellado. 1999. The chemokine SDF-1alpha triggers CXCR4 receptor dimerization and activates the JAK/STAT pathway. *FASEB J.* 13:1699–1710.

Wong, M., S. Uddin, B. Majchrzak, T. Huynh, A.E. Proudfoot, L.C. Platanias, and E.N. Fish. 2001. Rantes activates Jak2 and Jak3 to regulate engagement of multiple signaling pathways in T cells. *J. Biol. Chem.* 276:11427–11431. http://dx.doi.org/10.1074/jbc.M010750200

Zhang, X.F., J.F. Wang, E. Matczak, J.A. Proper, and J.E. Groopman. 2001. Janus kinase 2 is involved in stromal cell-derived factor-1alpha-induced tyrosine phosphorylation of focal adhesion proteins and migration of hematopoietic progenitor cells. *Blood*. 97:3342–3348. http://dx.doi.org/10.1182/blood.V97.11.3342

Zhou, Y.J., E.P. Hanson, Y.Q. Chen, K. Magnuson, M. Chen, P.G. Swann, R.L. Wange, P.S. Changelian, and J.J. O'Shea. 1997. Distinct tyrosine phosphorylation sites in JAK3 kinase domain positively and negatively regulate its enzymatic activity. *Proc. Natl. Acad. Sci. USA*. 94:13850–13855. http://dx.doi.org/10.1073/pnas.94.25.13850